ISSN/1120-5598

COMITATO NAZIONALE PER LA RICERCA
E PER LO SVILUPPO DELL'ENERGIA NUCLEARE
E DELLE ENERGIE ALTERNATIVE

Associazione EURATOM-ENEA sulla Fusione

AREA NUCLEARE

A HIGH PERFORMANCE AND LONG PULSE TOKAMAK

A. TANGA, M. ROCCELLA
ENEA - Area Nucleare, Dipartimento Fusione
Centro Ricerche Energia di Frascati

B.J. D. TUBBING, C.H. SACK
JET Joint Undertaking, Abingdon, Oxfordshire, UK

G. BOSIA
DG12, CEC, Brussels, (Belgium)

C. SBORCHIA
ANSALDO Ricerche, Genoa

Edito a cura dall'ENEA, Direzione Centrale Relazioni.
Viale Regina Margherita, 125 - Roma
Finito di stampare nel mese di giugno 1991
Fotoriproduzione e stampa
a cura della «Casa della Stampa»
Via Empolitana 120/C - Tivoli (Roma)

Questo fascicolo è stato stampato su carta riciclata

Abstract

A design proposal for high performance, long pulse, tokamak (HLT) is described. The main parameters of the machine are: major radius 3.4 m, minor radius 1.2 m, elongation 2. The maximum toroidal field on axis is 8.3 T, the maximum plasma current is 20 MA. The discharge flat top length is 40 s for a plasma with 20 MA inductively driven current at a toroidal field of 8.0 T, and 500 s for a discharge with 7 MA non-inductively driven current at a field of 3.5 T. In HLT the main physics issues for a fusion reactor can be assessed: plasma physics and plasma operation in the ignited and sub-ignited regimes; burn stabilisation; behavior of divertor components under long-pulse thermal loads; and semi-continuous operation with non-inductive current drive. The crucial element in obtaining this level of performance in a machine of medium size is the use of active cooling with liquid nitrogen both for the toroidal field coils and the central solenoid. The toroidal field coils have a pure copper conductor in a stainless steel casing. The stress in the copper does not exceed a, relatively conservative, limit of 180 MPa.

Riassunto

Viene descritta una proposta per il progetto di un tokamak (HLT) capace di elevate prestazioni e di impulsi di lunga durata. I principali parametri della macchina sono 3.4 m di raggio maggiore, 1.2 m di raggio minore, elongazione 2. Il massimo campo magnetico toroidale sull'asse è 8.3 T, la massima corrente di plasma è 20 MA. La piattaforma della scarica è 40 s per un plasma di 20 MA di corrente prodotti induttivamente con un campo toroidale di 8.0 T, e 500 s per una scarica di 7 MA prodotta mediante current-drive ad un campo toroidale di 3.5 T. Con HLT può essere data risposta ai principali problemi di fisica relativi ad un reattore a fusione: sulla fisica del plasma e sulla definizione delle procedure operative sul plasma nelle regioni ignite e sub-ignite; stabilizzazione della scarica nella fase di produzione d'energia, comportamento delle componenti nel divertore sotto il carico termico prodotto da una scarica di lunga durata; e realizzazione di un regime semicontinuo mediante current-drive non induttivo. L'elemento cruciale al fine di ottenere una macchina in grado di fornire questo livello di prestazioni è costituito dall'uso di un raffreddamento attivo con azoto liquido sia per il campo toroidale che per il solenoide centrale. Le bobine del campo toroidale sono costituite da conduttore di rame puro in una struttura di contenimento di acciaio. Lo sforzo nel rame non supera il limite, relativamente conservativo, di 180 MPa.

1. INTRODUCTION

In this paper a preliminary design proposal for a long–pulse, high performance tokamak (HLT) is described. The main physics parameters of the machine are listed in table 1, and table 2 gives an overview of the main engineering issues. Cross sections of the device are shown in figures 1 and 2. The main objectives of HLT are the demonstration of plasmas in ignited and sub–ignited regimes and the study of the main physics problems for a fusion reactor in conditions typical of a fusion reactor. This involves three major areas of work:

1) Achievement of a thermonuclear plasmas in the ignited regime, with characteristics similar to those of a fusion reactor.
2) Study of the methods of sustainment and control of the plasma burn, both in ignited and in sub–ignited regimes.
3) Demonstration of the feasibility of long pulse, semi–continuous operation with non–inductive current drive in thermonuclear conditions.

The choice of the main design parameters of HLT follows from the above points 1,2 and 3:

1) In order to produce ignited plasmas with temperature, density, and specific fusion power similar to the values needed in a fusion reactor one needs a tokamak of sufficiently large size, plasma current and toroidal field to obtain the minimum required energy confinement. With the basic parameters of HLT, namely a major radius of 3.4m, a toroidal field of 8T and a plasma current of 20MA, this condition is fulfilled.
2) In order to study methods of burn sustainment and control, the duration of the burn must be exceed the typical timescales of the physics processes that govern the burn. In HLT, the flat top pulse length of a plasma with 20MA inductively driven plasma current is 40s. In the sub–ignited regime, a plasma current of 15MA can be sustained for 90s. These times are sufficiently above the typical burn physics timescales to allow a realistic assessment of helium ash removal, impurity control and burn stabilisation. The ash

removal and the impurity control requires a pumped divertor system. HLT can be operated with top and bottom diverters, with pumping elements installed in the top and bottom horizontal ports.

3) In order to study quasi—continuous operation with non—inductively driven plasma current, a sufficiently long pulse length capability of the toroidal field must be available. In HLT, the toroidal field can be maintained at 3.5T for up to 500s. A toroidal field of 3.5T will allow plasma currents of about 7MA. The toroidal field pulse length capability can be extended at minot capital cost by increasing the size of the cooling energy reservoir. Long pulse operation can also be achieved with inductively driven plasma current. A plasma current of 7MA can be sustained by the central solenoid for about 200s with a loop voltage of 0.5V.

For HLT a substantial research programme with a deuterium—tritium fuel mixture is proposed. The total number of discharges is approximately 10000. It is an important aspect of the design, that the α power at ignition is not much higher than the total installed auxiliary heating power. This implies that discharge development and optimisation required for the D—T discharges can be carried out in plasmas consisting of deuterium or hydrogen.

The major experiments to be carried out in the maximum performance discharges (plasma current 15 to 20MA, toroidal field 7 to 8T) with a deuterium—tritium fuel mixture are:

a) Study of the heating path to ignition regimes with different heating methods. The optimization involves the use of different heating methods such as ICRH and/or NBI and schemes of plasma current profile control with LH current drive and stabilization of the plasma internal modes.

b) Study of the behaviour of enhanced confinement regimes at high power and in ignition conditions. This includes the H—mode confinement regime and the plasma regimes accessible with pellet injection.

c) Study and control of MHD instabilities. Of particular importance is the control of the internal mode, the external kink and the avoidance of plasma disruptions.

d) Study of the scaling of the plasma parameters at the ignition regimes.

e) Study of the ash removal and impurity control.

f) Study of burn stabilisation issues.

The topic f), ie. burn stabilisation, can be sub—divided in a number of experiments as follows:

f1) Exploration of soft beta limit conditions.

f2) Toroidal field ripple control.

f3) Variation of plasma density, plasma dilution or fuel composition.

f4) Variation of auxiliary power.

In the area of work of long—pulse and semi—continuous operation, major experiments can be carried out as follows:

a) Development of ICRH fast wave current drive.

b) Development of LH current drive.

c) Development of scenarios where the plasma current is driven in alternating direction by alternating current operation of the central solenoid.

d) The non—inductive current drive can be combined with the ignited plasma operation, in a mode in which the transformer is recharged by application of non—inductive current drive in periods in between successive burn phases. The advantage of this scheme is that during the current drive periods the plasma parameters can be optimised as regards current drive efficiency.

The parameters of HLT, shown in table 1 and 2 have resulted from an optimisation process aimed at combining some features of the construction of the JET device — such as the D shaped toroidal field coils, the active cooling, the additional heating predominantly based on ICRH and NBI —, with the characteristics of high—field tokamak — such as cryogenic liquid nitrogen cooling, moderately high value of toroidal field —, in an apparatus with moderate level of stresses and therefore with a high level of reliability and easy construction.

The design of the divertor relies on poloidal coil external to the toroidal coils. This is a requirement for reactor design. because it strongly simplifies design and serviceability of the coils. External poloidal field coils also produce high values of the poloidal connection length.

A basic principle is that of taking adequate safety margins in the design of major components. It will ensure a degree of flexibility as well as a future capability to exceed, if required, the basic design parameters. In the guidelines of HLT safety and environmental aspects have played a crucial role: first the choice of structural and shielding materials is such that the activation of the machine will be reduced to a few thousand curies after a 10 years cooling down period; second the size of the device is such that a moderately high building can accommodate it; third the assembly and disassembly procedures are made as simple as possible in order to reduce the cost of de—commissioning, and the problems of intervention in case of faults or accidents. As a concluding remark it should be emphasized that a considerable experience on technologies could be gained from HLT. As matter of course technological experience will be gained on all the high thermally loaded components of the divertor, as well as the elements of the machine exposed to neutrons, including some of the diagnostics. In parallel to the main physics program, a technology program can also be carried, consisting amongst others of the development and testing of small blanket modules that can be accommodated in the ports of HLT, and the development of helium pumping capability. The total neutron production of HLT is $2\ 10^{25}$ for the whole machine life. Conventional materials can be used for the construction; at the neutron fluences of HLT, no loss of strength or creep can be expected to occur for any metal. The toroidal field coils, however, need a neutron shield with a neutron energy attenuation factor of about 5, in order to prevent damage to the coil interturn insulation. It has already been stressed that the auxiliary heating capability of HLT is such that commisoning of discharge scenarios up to thermonuclear parameter regimes can be performed in deuterium or hydrogen plasmas. thus not producing significant activation of machine components.

2. OVERALL PHYSICS PERFORMANCE

2.1 Choice of the value of toroidal field

The choice of the value of the toroidal field of 8.0 T is due to three main considerations; First, with the value of 8.0T the values of $q_{\psi,95}$ is close to 4 at a plasma current of 20MA. In general tokamaks have obtained the best performance with q_{ψ} between 3 and 4, where the central instability region is smaller than half the plasma minor radius. The sawtoothing instability can therefore be stabilized possibly for the entire duration of the high current flat top by a moderate amount of current drive or by possible effects of fast particles [1]. Second, the relative high value of the toroidal field ensures an adequate margin on q_{psi} if the value of the plasma current needed to be increased further. Third, the 8.0T toroidal field allows a larger operational space on the side of high fusion power by virtue of the ratio β/β_{crit}.

2.2 Preliminary considerations on plasma performance.

A first point to be made for predicting the physics performance of HLT is that, from the point of view of the plasma geometry, the plasma dimension are similar to that of JET. A first strong simplification can therefore be made in the predictions because one can , in first approximation, base an extrapolation to 20MA and 8T just on JET results. One simple way of proceeding is to extrapolate the scaling obtained on the basis of the results of the JET H—mode , with the assumption, which is justified later, that HLT can achieve an H—mode with characteristics similar to that of JET. The ratio between α power and plasma loss power can be written for a 50—50 deuterium—tritium plasma in the appropriate range of temperature, assuming equal electron and ion temperatures as:

$$F = 3.2\ 10^{-22}\ \hat{n}\ \hat{T}\ \tau_E\ f^2\ y\ /\ (2y-1) \qquad (1)$$

where $\hat{n}$ and $\hat{T}$ are the central values of electron densities and of the plasma temperature, τ_E is the value of

the global energy confinement time , f is the dilution factor (the ratio between the ion and electron densities), and y is the pressure peaking factor (the ratio between the central value of the plasma pressure and its volume averaged value). At ignition one has that the α power balances the plasma power losses and the value of F is unity. For values of F above unity the α power exceeds the transport losses and one has a margin above ignition, while for values below unity the device does not have an ignited space of parameters. Rewriting eq. 1 one obtains:

$$F = P(MW)\ \tau_E^2\ f^2\ y^2\ /\ (1.5\ V(m^3)\ (2y-1)) \qquad (2)$$

By substitution in formula 2 of the values of the scaling of the JET H—mode global confinement time, as reported in references [2] and [3] one obtains the values for F reported in table 3. There is a good margin for ignition for both of the cases shown. The first column refers to values of dilution of 0.8 and pressure peaking factor of 4 and the second refers to values of dilution of 0.9 and pressure peaking factors of 5. It should be noted that the above values have routinely been exceeded in JET H—mode operations. Especially recently with pellet fueled discharges the values of pressure peaking factor achieved were of the order of 7, with an estimated dilution of 0.95.

2.3 H—MODE CONDITIONS FOR HLT

It should be emphasized that operation with pump divertor are designed to achieve control of plasma density and impurity influxes even in ignition regimes. Consequently a substantial improvement compared to present JET H—mode conditions should be achieved. In JET the condition for the H—mode transition are the presence of a magnetic separatrix and a value of the additional power above a certain threshold [4,5]. It has been found ,in JET and in other tokamaks that the main dependence for the threshold power is an approximately linear increase with the applied toroidal field [5]. If one scales the JET values to HLT,one obtains a power threshold of 30MW for a value of toroidal field of 8.0T, well within the capability of the HLT heating system.Without a purpose built pump divertor the duration of the ELM free JET H—mode is equal to ~

the time that the radiation losses take to reach the input power.This happens with a continuous rise in plasma density. an influx of impurity larger than the outflux, the rate of increase of the radiation has a slope of 1—2MW/s.[6].It could be therefore expected that even without a beneficial divertor action, the duration of the H—mode to last for times comparable to the duration of the available high performance flat—top length.The maximum density at which the H—mode can be sustained also depends on power radiated by the bulk plasma. In JET such density scales as ,$<n>(m^{-19})=2.12\ P^{0.5}(MW)$, where ,.<> denotes volume average, for a series of JET 3MA discharges. with gas fueling, while with pellet fueling the limit is substantially higher.Again in HLT a higher proportionality factor could be expected.Even assuming no improvement and the above simple power scaling one obtains $<n>=1.5\ 10^{20}\ m^{-3}$ for the lower power of the sub—ignited regimes and $<n>=2.12\ 10^{20}m^{-3}$ for the higher power of the ignited regimes.

2.4 BURN CONTROL

The experiments on the control of the plasma burn have two main inter—related aspects; 1)Control of the α power; 2)Removal of the Helium ashes. These two aspects are closely related because the time scale is similar for both and because the ashes accumulation itself causes a moderation of the burn phase and at high Helium concentrations, the switch—off of the burn. Fueling the discharge is done with three standard methods : gas fueling with simple puff valve is effective but probably inefficient with strong particle fluxes directed toward the divertor, neutral beam injection produces fueling as well as heating and tritium injection is planned for present generation tokamaks. peilet fueling is very reliable and with high efficiency; if central pellet deposition is required in ignition regimes, the present generation of injectors are clearly inadequate.The control of plasma density is performed by a pump divertor, it has an estimated pumping speed of 10^6 l/s. While there is evidence of Helium pumping by the Beryllium surfaces in JET [7],for HLT helium pumping is certainly a critical area of research.The crucial plasma parameter for ash removal and burn control is the ratio between the particle effective diffusion coefficient and the the values of the thermal conductivity. The value of this ratio should be sufficiently large to ensure low residence fraction of the Helium particles in the discharge with at the same time a sufficiently energy confinement properties to be able to sustain the ignition regime.

Several active and passive methods have been proposed for burn control. There is immediately a major difference to the problem of plasma burn control for ignition or sub—ignited regimes: the ignition regimes are thermally unstable , while the sub—ignited regimes can be thermally stable.It should be noted that apart from the complication of the ash removal, in practice many other plasma phenomena should be expected to play a non irrelevant role. The sawtoothing activity, when present will modulate strongly the fusion power, by modulating the central values of plasma temperature and density, and possibly by perturbing the orbits of the α particles.A second possibility of plasma perturbation is that one of ELMS, for an H—mode ignition, en ELM causes a temporary reduction of energy and more pronounced increase of particle transport. One could think about schemes which could control some of these instabilities as a possible way of burn control, or modulate the pumping of ashes via for example a variation of conductance plasma—pump divertor done for example by radial weeping of the X—point. If some of these mechanisms are seriously affecting the plasma confinement, then they will limit the value of Q and all depends on the effective merits of each method, but technically speaking succeeding in controlling the plasma burn means operating in a sub—ignited regime.The sub—ignited regime can be thermally stable and then one of the most effective ways of burn control can be done by modulating the additional power. The crucial parameter of these experiments is the value of Q and the extrapolation to a reactor based on economic considerations.

2.5 LONG PULSES—QUASI CONTINUOUS OPERATION

The technical feasibility of long pulses , of the order of 500s at a value of toroidal field of 3.5T, depends in HLT on an efficient current drive. Assuming the use of LH current drive and scaling the results form those of experiments, it can be estimated that in order to drive plasma current of the order of 7MA , a total radio—frequency power of the order of 30MW at frequency of 6 to 8GHz could be required. In these conditions the average value of plasma density can be 5 10^{19}.In this regime it can be expected that plasma performance will be of the order of break—even, as scaling from JET.

Apart from the use of LHCD one can expect to be able to drive plasma current also by the use of a suitably phased array of ICRH antennas and by bootstrap currents. From the point of view of the experiments, main points are:

1) Study of current drive in multi—mega—ampere plasma for very long pulses

2) Study of the ash removal, or helium pumping under large integral thermal and particle load.

3) Development of diagnostics and plasma control systems for those long pulses.

2.6 PLASMA STABILITY

The study of plasma instabilities is very important in HLT. As it has previously been emphasized the control of specific instabilities has a crucial role in the burn control. The avoidance of plasma disruptions is important to reduce the stresses on the in vessel components. An estimate of the forces acting on the vessel of HLT due to vertical instability can be done scaling in plasma current the values observed in JET. Assuming that the observed quadratic scaling can be extrapolated to HLT one obtains a value of 10000tons, which will betaken by the 32 toroidal coils. The force acting on each has however to take into account a certain degree of toroidal asymmetry, as observed of the order of a factor of 2.

3 COMPUTER CALCULATION AND SIMULATIONS OF PLASMA PERFORMANCE

The plasma performances of HLT have been preliminary calculated by 1/2D computer code [8] and by 1 1/2 D computer code JETTO, using different models for the transport. The main results of the 1/2D computer code calculations are shown in figs 3,4 and 5 obtained by using the Rebut—Lallia scaling [9]. The Rebut Lallia scaling does not really represent the H—mode confinement, however the confinement obtained in the JET H—mode is approximately a factor 1.5 better than the Rebut—Lallia scaling would predict. The three plots show the POPCON contour for 20MA HLT with the assumption of values of Z_{eff} of 1.0, 1.5 and 2.0, assuming as impurity a mix of Oxygen and Carbon. The plasma density profiles are assumed to be parabolic to 0.5, while the parabolic temperature profiles are flattened in the central half of the radius assuming strong

sawtoothing.The values of the beta limit has been taken according to a Troyon scaling with a multiplier of 2.8, the lower curve takes into account the contribution of the α particles.The axis are the central peak values of plasma density and temperature. It is shown that there is a wide ignition region at all the above values of Z_{eff} for peak densities above 2 10^{20} and for peak temperatures above 10 kev, which is a value which is routinely achieved in JET

The minimum value of the α particles power on the ignition boundary ranges between 20MW for the z_{eff} =1.0 case to 100MW for the case with z_{eff} =2.0. The code has been run by using the ITER H—mode scaling [3] already mentioned in the previous section which also has a wide ignition region.In the latter case the minimum values for α power range between 10MW and 50MW depending on the value of Z_{eff} For both scalings the additional power needed to access the ignition region is far below the planned 40MW of HLT.

Without the H—mode improved confinement runs obtained with the Kaye—Big—Complex scaling, based mainly on the confinement results of the L—mode discharges of JET,TFTR and JT60, the results of the 1/2D code still show the ignition as marginally possible, always with the same assumptions as before, but with Z_{eff} equal to 1.0.

With the 1 1/2D code JETTO simulation runs of the plasma behaviour of HLT have been performed. The code uses full flux geometry as derived from runs of the plasma equilibrium code.

First an ohmic case is run until an a steady state is reached. The results of the ohmic calculations are then fed into a new run in which the additional heating is switched on. A series of simulations have been performed with several local transport models. since a set of local transport coefficients is not yet available for simulations of H—mode discharges, the models used are more appropriated for L—mode discharges.The results of the simulation essentially are in good agreement with the results of the calculations done with the 1/2 D code, reported earlier.In the following figures from 6 to 21 an output result is shown for a run with plasma current of 20MA, toroidal field of 8.0T The run was done using the Lackner—Gottardi scaling+profile consistency constraints [10,11] . The run start from an Ohmic steady—state at time 20s, at which an additional heating power of 20MW of Deuterium beams are switched on into a target plasma composed equally of Deuterium and Tritium. As consequence of the additional heating the plasma density increases and the α and total power also increase. after 15s the NBI injection is switched off while the plasma is undergoing a full ignition. In fig 9 the

time evolution of the ratio between the total fusion power and the input power Q_5 is shown. Evidently the ignition regime corresponds to the value of Q_5 equal to 5, which corresponds to the values of F=1.0 of the previous section. The ignition is reached in this case after 15s of NBI heating and the value of the fusion power is in this case stabilized and modulated by the sawtooth activity.Fig 11 shows the time evolution of the central value of q as calculated by using Spitzer resistivity and neo—classical corrections. A sawtooth reconnection is triggered when the central value of q drops below 0.8.The reconnection is simulated with the Kadomtsev model, and the central value of q is restored to the value of unity.In the case under consideration the sawtooth period is of the order of 5 seconds. The time evolution of the values of the global confinement time,Z_{eff} and resistive loop voltage are shown in figures 12,13 and 14 respectively.While the evolution of the plasma temperature is mainly determined by the energy transport model, the evolution of the plasma density profile is determined essentially by the particle transport model. In fig 15 three plasma density profiles are shown , the particle local transport model used here has been obtained by fitting the plasma density evolution in high current JET pulses.The flow of particles is dominated by a diffusion coefficient $D = 0.1\ \chi_e$ the inward pinch term produces only a 10% contribution to the particle flux. Consequently, as shown in fig 15 the plasma density profiles tend to be rather flat with most of the plasma density gradient concentrated in the outer 20% of the plasma flux equivalent minor radius.The deposition profile of the 140keV NBI for these values of plasma density is rather broad and does not contribute significantly to the shape of the plasma density profile. Radial profiles for electron and ion temperatures are shown in fig 16 and 17 at the peak of the sawtooth period. The toroidal current profile density is shown in figs 18 and 19 . Fig 19 shows the radial profile of the bootstrap current contribution. Fig 20 shows radial profile of the D—T reactivity Fig 21 shows the time evolution of the poloidal and toroidal beta, please note the factor 10 on the scale of the toroidal beta.

4. OPERATIONAL SCENARIOS AND NEUTRON PRODUCTION

In this section the three main reference operational scenarios for HLT are summarised. The main parameters of these scenarios are shown in table 4. The first, type A, is the discharge type of maximum fusion performance, for which the ignition predictions have been carried out. Discharge type B, which has a plasma

current of 15MA and a toroidal field of 7T. with a pulse length of 90s, is the reference scenario for the development of sub–ignited burn control strategies and for the development of ash removal and impurity control techniques. Discharge type C, with a toroidal field of 3.5T, sustained for 500s, provides the basic plasma on which to carry out the development and optimisation of long pulse and semi–continuous operation scenarios.

The neutron production of the discharge types A and B, calculated from the expected fusion power, and assuming an average duration of burn, is also shown in table 4. The total neutron production during the lifetime of HLT was estimated on the basis of these numbers. A D–T programme, with a total duration of six years is assumed, with a number of operational days of 100 per year. It is further assumed, that per operational day not more than 4 discharges of type a or B can be run (these discharges require the full capability of the cold storage). In addition a number of smaller discharges, say 10, producing 1.0 10^{21} neutrons each, can be run per day. A total number of pulses of about 10000, with a total neutron production of about 2 10^{25}, then appears as a realistic estimate. This should be compared with the number of 10^{24} predicted for the JET D–T phase [12], where it should be noted that JET has no neutron shielding. In table 5 the neutron production, the total neutron fluence and the total neutron energy are summarised. Table 4 also shows the power supplies and cooling energy requirements for the toroidal field coils for the three discharge types. The cooling system will be described in section 6.

5. MAIN ASPECTS OF THE ENGINEERING

The main components of the load assembly of HLT are shown in figure 22. In this and the following sections. the considerations leading to the particular design, and some details of the construction, will be described.

The conceptual design of the engineering of HLT follows logically from the stated physics objectives. The objective of obtaining a long pulse capability, with conventional copper toroidal field coils. leads naturally to the concept of coils operating at liquid nitrogen temperature, and being actively cooled with a pressurised liquid nitrogen system (see next section). The long pulse capability is further obtained by using a central solenoid of relatively large outer diameter, and by strongly cooling the central solenoid with a similar cooling system. It

should be noted here that the cooling, rather than the stresses, dominates the design of these coils for long pulse applications.

The toroidal field coils of HLT basically operate in pure tension, but they have a transition in the tensile stress at the highest and lowest points of the coil. This construction allows the inner radius of the toroidal field coils to be larger for a design which operates in pure tension without a transition. Furthermore, a higher elongation of the TF coil can be achieved, thus making space for an elongated plasma and for divertor components, and the tensile force along the inner leg of the coil can be reduced. With the coils of this shape, the vacuum vessel can be built close to the coil everywhere.

In order to be able to sustain a substantial program in deuterium—tritium, a neutron shielding has been applied between the TF coils and the first wall. The thickness of the shield is between 100 and 150mm, and the shield consists of a suitable high Z material. The shield, and the vacuum vessel, are water—cooled. The minimum required neutron energy attenuation of the shield is factor 5 along the inner—wall. The functions of the shield are to reduce the nuclear heating of the TF coils, to prevent significant degradation of the coil inter—turn insulation, to prevent the resistivity of the copper to increase under the accumulation of neutron—induced lattice defects, and to reduce long term activation in coils and surrounding materials.

For the vacuum vessel and associated stiffening components, preferably a low—activation material should be used. The requirement is that the induced activation of the vacuum vessel, after a 10 year cooling down period, should not significantly exceed the activity induced in other machine parts, in particular TF coils and shielding material. No final choice of material has been made yet.

The TF coils of HLT are made of steel cased, high purity oxygen—free copper. The choice to use this type of coil, rather than full copper coils made of a strengthened copper (Glidcop copper with aluminium—oxide or beryllium—copper), was made on a number of considerations: first, at liquid nitrogen temperature, and with coils that are actively cooled, maximisation of the cross—section is less of an overriding consideration than for passively cooled coils (where heat capacity is important); second, the decrease of copper resistivity with decreasing temperature is larger for pure oxygen free copper than for the strengthened coppers; third, cased toroidal field coils are naturally much stronger against the out of plane bending forces; fourth, cased coils can at the same time function as the main structural element of the machine. Cased coils, with a bolted on mechanical

structure, will allow for easier coil replacement than full copper coils that are supported by an external structure. The cased coil concept also relates more closely to super—conducting coils. It is possible, in principle, to replace one or more of the coils of HLT by super—conducting equivalents.

The machine is build—up of 16 identical sectors, where each sector contains two TF coils, and a sector of the vacuum vessel including a major horizontal port. The two TF coils in one sector are connected with a shear panel that takes the overturning and out of plane bending forces. Coils in neighbouring sectors are connected via a system of bars. The sectorisation has advantages over a system in which the machine is build of a smaller number of larger elements, in particular in view of the substantial D—T program. A sector is a relatively inexpensive item. Rather than having to carry out major repairs on a radioactive sector (with remote handling tools that would represent an expensive investment), the sector can be replaced in its entirety. The weight (about 50ton) and size of the sectors is such that road transportation is not a big problem. The system of cased coils with bolt—on bars allows for 16 major horizontal ports protruding between the bar connections. A number, say 4, of these ports can be permanently dedicated, or made easily accessible, for remote handling apparatus. In this way, remote handling tools will have to have only a limited reach around the machine, which limits their size and cost. Horizontal ports at the top and bottom of the machine are accessible to remote handling tools for the servicing of divertor components.

6. ACTIVE LIQUID NITROGEN COOLING

In this section it will be argued that the concept of active cooling with liquid nitrogen of both the TF coil set and the central solenoid is a crucial ingredient in achieving the high current and long pulse capability in a machine of medium size.

The resistivity of copper at an operating temperature of about 100K is reduced by about a factor 6 with respect to that at room temperature. The strength (ultimate tensile and yield strengths) of copper and steel are increased by about a factor 1.5 at these temperatures. Furthermore, creep of copper is eliminated.

In designing liquid—nitrogen cooled TF coil sets, one has to make the basic choice between an inertial cooling system (in which the coil is cooled to 70K before the plasma discharge, and heats up to room

temperature during the discharge), and an active (steady—state) cooling system, where a low operating temperature is maintained in steady—state operation up to the maximum coil current. In HLT, the TF cooling system is steady—state. This has the following advantages with respect to an inertial system: first, the resistive power required to drive the coil current is maintained at a constant low level (400MW in HLT) throughout the discharge, whereas in an inertial cooling system it would rise by a factor of about 6 during the discharge(for an inertial system, the coil design would be somewhat different, but the required power would be at least of order 1GW); second, the total resistively dissipated energy is minimised for a given pulse length; third, the increased strength of the materials is retained throughout the discharge; fourth and most important, the maximum TF pulse length is now determined solely by the amount of cooling energy available in a cold storage facility. The cooling system of HLT consists of a 20bar pressurised liquid nitrogen closed loop operating between 70 and 110K, which is heat—exchanged against a large liquid nitrogen storage facility at 1bar and operating between 65 and 75K. Figure 23 shows the concept. The size of the reservoir should be of order $2000m^3$ (see next section). The cooling pumps will operate only during tokamak discharges. The steady—state cooling power of the cooling plant, calculated on the basis of the assumption that the equivalent of 6 discharges requiring maximum cooling energy (type A, see table 4) can be run per day, is about 2.5MW, assuming that the plant works 24 hours per day.

Operation of the coils at 100K allows relatively high current densities (up to $55MA/m^2$ is used). This allows for a compact coil conductor ($0.08m^2$ on high field side part of the coil), surrounded by a steel casing. The steel casing takes about 50% of the tensile force along the high field side of the coil. The most important function of the casing is however not to support the tensile force (this could also be done by increasing the copper area, at the expense of having a slightly larger coil), but to support the coil against inter—turn shear, arising from the out of plane bending forces due to the poloidal field crossing with the coil current. These forces are particularly severe in divertor machines with divertor coils external to the TF coils. Also, the casings in HLT are used directly as the main structural elements of the machine; vacuum vessel, shaping coils etc. are directly supported on the casings.

Design of a cooling system for the central solenoid is more constrained than that for the TF coils, where the reduction of conductor strength due to the cooling holes can be compensated for by adding casing material.

The central solenoid, at high current, is subject to expansion forces, which are partly balanced by TF centering pressure, and partly by tensile hoop stress in the copper. Any further strengthening material can only take the form of a shell between the solenoid and the TF coils, which is very unfavourable from the point of view of aspect ratio.

The central solenoid of HLT uses a combination of active and passive cooling. Currents up to about half the maximum current (stress limit) can be run in steady state, with the copper temperature not exceeding 100K. Higher currents cause the coil temperature to increase, up to the maximum value of 110K. The cooling system will, during the plasma formation phase when the coil current goes through zero, remove the heat generated in the coil during the pre–magnetisation phase. The required cooling power in the HLT design is determined by the consideration that for a plasma of 20MA plasma current, the coil will reach the maximum temperature at the same time as it reaches the stress limit, ie. after a flat top of 40s.

It would clearly be very difficult to construct a central solenoid with water–cooling that would meet these specifications. Because the size of the central solenoid can not be increased without increasing the machine size, the dissipation at room temperature would be about 6 times higher.

In summary, the high–power liquid nitrogen cooling is essential for the achievement of high–current and long–pulse capability with a limited machine size. The total energy demand from the grid will not be much reduced with respect to a water–cooled similar machine, because the efficiency of liquid nitrogen production approximately cancels the gain made in copper resistivity. However, the maximum power demand is much reduced. Even allowing for the fact that in a water–cooled design the coils would have a larger conductor cross–section, the saving in resistive dissipation is at least a factor 2 to 3 (Compare eg. HLT with 400MW at 8.3T to JET with a dissipation of 270MW at 3.5T [13,14]). The reduction of the peak power results in lower cost of operation of the machine, and in a wider range of options for the siting of the machine.

7. ASPECTS OF THE CONSTRUCTION

The main components of the load assembly are shown in figure 22. In this section, the various elements will be described in some detail.

Toroidal field coils. The main parameters of the toroidal field coils are summarised in table 6. The number of toroidal field coils is 32. The coils are of the well–known bending–free shape [15], where the dominant force on the coil is a tensile force, constant along the arc. There is a transition in the tensile force at the highest and lowest points of the coil, such that the tensile force along the high field side part of the coil is reduced. This transition serves two purposes: first it allows for coil shapes with high elongation (when inner and outer radii of the coil are given), to match highly elongated plasma shapes and leave space for divertor components; second the reduced tensile force along the high field side part allows for a smaller coil cross–section, which benefits the machine aspect ratio. Figure 24 shows the main dimensions of the TF coils. Figure 25 shows the tensile force as a function of coil arc distance, for the case of the maximum current of 4.4MA in the coil, which corresponds to a field of 8.3T at the machine major radius of 3.405m. The resultant force across the transition is taken by a structural element in the form of a ring, the crown. These rings can be seen in figure 22. They are made of laminated stainless steel, bonded with epoxy, in order to prevent eddy currents induced by the poloidal circuit. In order to prevent high shear stresses between the turns and the casing, the transition in tensile force is not abrupt, but is spread over an arc length of 1m. In this transition region, the turns will be keyed to the casing.

The conductor is oxygen free, high–purity copper. The coils are tape–wound (as opposed to the pancaked coils used in JET [14]). The advantage of tape–wound coils is that the winding exhibits a high stiffness against the out–of–plane bending forces, resulting from crossing the coil current with poloidal fields. These forces are particularly strong in the divertor region. The conductors are contained in a stainless steel casing, which provides 50% to 70% of the tensile strength of the coil. The casing eliminates the problem of inter–turn shear forces on the insulation, which, on a relatively small, high field machine, is potentially serious. Figure 26 shows cross–sections of the coil at the high and low–field side mid–plane respectively. The areas of conductor, casing, cooling holes and insulation are indicated in the figure. The maximum axial tensile stress in the copper

conductors is about 180MPa, the maximum stress in the stainless steel casing is about 360MPa.

The TF coil casings form the main structural element of the machine. They provide support for the poloidal field coils and the vacuum vessel. The machine is sectored in 16 identical sectors, each consisting of two TF coils with associated vessel elements. The two TF coils in one sector are connected by shear panels, which resist the overturning moments. Connections between neighbouring sectors are made simply by bolt—on bars, leaving space for 16 major horizontal ports.

The TF coils are actively cooled with a 20bar pressurised closed loop liquid nitrogen cooling system. Cooling calculations, assuming circular cooling holes with a total hole area of $0.04m^2$ (256 holes of 14mm diameter) in the coil cross—section were performed, using the Dittus—Boelter equation $Nu = 0.023\ Re^{0.8}\ Pr^{0.4}$ [16] between the Nusselt, Reynolds and Prandtl numbers. The calculations show that with a fluid speed of 5m/s, and fluid entry temperature of 80K, the cooling power equals the maximum dissipated power (at the maximum coil current of 4.4MA) at an operating temperature of about 105K. The boiling point of nitrogen under 20bar is 115K, hence no boiling of nitrogen should take place. The pressure drop across the coil for this system is about 0.8bar. The installed liquid nitrogen pumping power is about 1MW for the total TF coil set. The cooling holes for the TF set should be internal to the conductors, in order to prevent contact between the coolant and the insulation.

The liquid nitrogen in the closed loop system will be heat exchanged against the low temperature cold storage facility. The size of this pool determines the maximum flat top duration for the toroidal field. For a cooling energy demand of a maximum performance tokamak pulse of order 36GJ, the size of the reservoir should be about $2000m^3$ of liquid nitrogen (heat capacity 2kJ/(kg K).

The resistivity of high—purity copper at 100K is about $3.15\ 10^{-9}\Omega m$. The total resistance of the TF coil set of 32 coils, with 22 turns each, is about $10m\Omega$. The dissipation at the maximum coil current of 200kA is then about 400MW, and the resistive voltage drop is 2kV. The inductance of the coil set is about 600mH. The maximum magnetic stored energy is 12GJ.

With a peak power demand of 600MW, and a maximum voltage of 6kV, a TF rise time of about 40s from 0 to 8.3T can be achieved. For a TF flat top time of 40s at 8.3T, the integral power demand from the power supplies is about 41GJ.

The situation may arise that the cooling system fails during a discharge, and that, due to a failure of the electrical system, the inductive energy is fully dissipated in an un—cooled coil. With a heat capacity of a coil of about 3.5MJ/K, this situation will lead to a temperature rise of about 110K. Although this will lead to total evaporation of the liquid nitrogen in the coil, and to an emergency release from the 20bar system, there is no danger to the integrity of the coil (the main danger being differential thermal expansion between the copper and the casing).

Central solenoid.

The central solenoid in a tokamak is subject to two main forces: the centering force from the toroidal field coils, and the expansion force due to the current in the solenoid itself. In HLT, as in JET [14] the centering force, in the absence of solenoid current, is taken by compressive hoop stress in the central solenoid itself plus an internal steel cylinder, mounted inside the solenoid. When current is passed through the solenoid, the expansion force is balanced by the centering force from the toroidal field coils, and by tensile hoop stress in the central solenoid. When in expansion, the solenoid can separate from the internal steel cylinder. This mode of operation is well—known from JET.

The central solenoid is separated from the toroidal field coils by a structural element, the central shell. This is a shell of 50mm thickness, in which the TF coils engage via vertical grooves. The shell is made of laminated stainless steel, epoxy bonded, so that a structure results in which no eddy currents will be generated but which still has a high stiffness against torsion. The central shell thus supports the TF coils against out of plane bending forces, but does not restrict vertical movement of the TF coils. The pancakes of the central solenoid are also locked to the central shell via a system of grooves, to prevent rotation of the pancakes. In the case of net expansion of the central solenoid, the shell works in expansion.

The stress distribution in the materials of the central solenoid was calculated using a simple model. The radial build—up of the model is shown in figure 27. The solenoid is assumed to consist of a number of concentric cylinders of steel, copper and insulation. The differential equation for the displacement under stress is solved analytically inside each material, taking into account the magnetic body—force acting on the copper

shells. At each interface between materials, the boundary conditions are applied of constancy of radial stress and of radial displacement. At the outer boundary, the centering pressure of the TF is applied as a boundary condition. The increase in the stresses in the copper due to the presence of cooling holes was taken into account by applying a weakening factor to the copper. The inter—turn insulation is lumped in 2 thick layers, instead of the 8 or 10 thin layers in reality.

In table 7 the stresses in the different elements are summarised for the compressive loading case, in which there is maximum centering pressure from the TF and no current density in the central solenoid. The composite stresses are calculated according to the maximum shear strain energy algorithm, where $\sigma_{composite} = ((\sigma_r - \sigma_z)^2 + (\sigma_z - \sigma_t)^2 + (\sigma_t - \sigma_r)^2)/2$, with σ_r, σ_z, σ_t the radial, vertical and tangential (hoop) stress respectively. Note that vertical stresses are neglected in the calculation, and also that all elements are assumed to be at the same temperature. We see from the table that the copper stress does not exceed 150MPa. The stress in the inner steel cylinder is maximum at the inner radius of the cylinder, at 325MPa.

In table 8 the same stresses are summarised for the case of expansion, ie. maximum TF centering pressure and maximum current in the solenoid. Note that this implies that the TF field should be maximum if the maximum flux swing is to be used, and that at lower field the maximum solenoid current is reduced. The maximum composite stress in the copper is now 176MPa, at a current density of 45MA/m^2. In the approximation of an infinite solenoid this corresponds to a flux of 98Wb.

The cooling system for the central solenoid is a 20bar pressurised liquid nitrogen closed loop cooling system, heat exchanged against the cold storage reservoir. The solenoid will be constructed out of a number of pancakes. Cooling holes will go vertically through the pancakes, thus cutting through the inter—turn insulation. Cooling manifolds will be located at the top and bottom of each pancake. The operating temperature range of the central solenoid is between 70 and 110K. Preliminary calculations were carried out of the cooling system of the central primary, in which the primary current was calculated from the required plasma current for a given plasma inductance and a given mutual inductance between plasma and solenoid. The flux induced by the vertical field equilibrium coil was taken into account.

These calculation are summarised in table 9 and figure 28. They indicate that for a 20MA plasma with a 20s rise time and 40s flat top, with a pre—magnetisation current in the coil equal to the maximum current given by

the stress limit ($45MA/m^2$), the stress limit and the cooling limit for the coil are reached simultaneousiy at the end of the flat top. The fluid speed for this system is 8m/s, and the fraction of cooling holes in the volume is about 10%.

For lower toroidal fields, the maximum current is lowered proportionally and the solenoid is operated at reduced stress levels. Similar calculations show that for a 15MA plasma with a 20s rise time and a 0.2V loop voltage, the maximum permissible temperature is reached after about 90s, with a maximum current density of $37MA/m^2$ in the coil. Note that these calculations were performed in order to establish the basic parameters of the cooling system, and that the model for flux consumption does not take into account the stray fields and shaping currents, which give an additional contribution to the magnetic flux.

With these cooling system specifications, a solenoid current of $27MA/m^2$ can be run is steady state.

Vacuum vessel and shielding. The shape of the vacuum vessel and the location of the main ports is shown in figure 22. The distance between the first wall and the TF coil is 200mm on the high field side, and 150mm on the low field side. The vessel centre is at 3.405m, and the horizontal internal diameter of the vessel is 2.47m.

There are 16 main horizontal ports, situated in the toroidal location between TF coils which are connected by the bar connections. The dimensions of these ports are: height 1.5m, width 0.35m. These are the main ports for auxiliary heating systems, diagnostics and remote handling. In the remaining 16 midplane locations, where the TF coils are connected by shear panels, there are smaller penetrations leading to spaces for 16 midplane Ion Cyclotron Resonance Heating antennas.

There are 16 upper and 16 lower horizontal ports, with an internal width of about 0.2m and a height of 0.5m. These ports, which have no direct line of sight through the plasma centre and can be well shielded from the neutron flux, contain the cryo—pumps for the divertor pumping, and allow access fir installation and servicing of divertor components. In addition, there are 32 upper and 32 lower vertical ports, with a toroidal width of about 0.1m and a poloidal width of about 0.2m. These ports are used for vessel suspension.

The vacuum vessel is surrounded by a neutron shield. The function of the shield is to absorb most of the neutron energy, in order to limit nuclear heating of the TF coils set, to prevent neutron damage to the coil inter—turn insulation, and to prevent an increase of the copper resistivity under the neutron fluence [17]. The

specification for the shield is that the total neutron energy fluence on the TF coils should be reduced by at least a factor of 5 with respect to the fluence at the first wall ($6\ 10^{22}\ m^{-2}$ neutrons at 14MeV). With this level of shielding, and the use of advanced insulator materials (eg. boron–free glass cloth with a poly–imide filler), it is expected that no serious degradation of the insulation should take place, while the increase of copper resistivity is estimated to be less than a few percent. At the high field side, the shielding thickness is 150mm, while at the low field side, where the fluence is lower, the thickness is 100mm. The shielding consists of a suitable high Z material. Candidates are lead or tungsten, in the form of pellets (Note that tungsten can, in principle, also be used as a structural material, in the form of plates or bars with bolted connections. It is, however, difficult to combine with other materials due to the very low coefficient of thermal expansion, $4.5\ 10^{-6}$/K). The shielding material will be contained in box sections that also serve to stiffen and re–enforce the first wall.

The shield and vessel absorb most of the plasma energy loss (including the nuclear energy), and hence they must be cooled. In order not to add to the total demand for liquid nitrogen cooling capacity, vessel and shielding will be water–cooled. The operating temperate will be between 10 and 80°C. The temperature difference between vessel and TF coils requires thermal insulation, and poses a problem of differential thermal expansion. Therefore sectoring of the vessel is required, with poloidal bellows separating vessel sectors. The sectoring is shown in figure 22. Each set of two TF coils carries a vessel sector of $2\Pi/16$ toroidal circumference. The bellow (this is also the line along which the vessel will be cut in the case of sector removal) is parallel to and near to the nearest TF coil, so that it does not cut through ports or ICRH antenna slots.

A final choice as regards the first wall and vessel structural material has not yet been made, mainly because the essential but complicated calculations of residual activation and tritium inventory have not yet been carried out. Candidate materials, which satisfy basic criteria of cost, fabricability and vacuum compatibility, are stainless steel, aluminium and titanium (alloyed). Of these, aluminium and titanium are low–activation materials [18]: it was estimated, on the basis of data form JET [19], that after a 10 year cooling down period after termination of the D–T research program, the residual activity would be of order 20000Ci for a stainless steel vessel, 1000Ci for an aluminium vessel and 100Ci for a titanium alloy vessel. These numbers will have to be compared with residual activation levels for the TF coils (dominated by the stainless steel casing, estimated 1800Ci after 10 years), and the activation of the shielding material. A material choice is

acceptable if the residual activity of the vessel does not significantly increase the total machine activation, and hence the de—comissioning cost. Other considerations are the strength of the material (stronger materials allow smaller constructions and hence less penetration of the shielding), thermal expansion coefficient (aluminium with a high coefficient of thermal expansion will require a larger expansion gap between vessel and coils), Thermal conductivity (aluminium with a high heat conductivity will allow most of the in—vessel components to be cooled through the first wall, thus simplifying construction), and tritium compatibility. In particular titanium forms a hydrate and has a high diffusivity for hydrogen. If titanium is selected as first wall material, a diffusion blocking surface layer must be applied (eg, a thin gold plating).

The weight of the vessel will be about 350ton. The weight will be supported via the vertical ports. These will be connected to the TF coils via spring assemblies which will absorb the differential expansion between vessel and coils and the deformation of the TF coils under the magnetic force. The stiffness of these springs will be such that at the maximum relative displacement between vessel and coils an acceptable stress in the vessel results. These springs will be insufficiently stiff to support the vessel against disruptions.

The vessel movement should be further constrained in the case of disruptions, to prevent a direct impact of the vessel against the TF coils. During disruptions, a force of order 10000ton occurs between the vessel and the TF coils. (The value of this force was discussed in section 2.6). It would be impracticable to transfer such a large force to the TF coils via the ports. A solution was adapted in which the vessel motion is constrained by a large number of disc springs, mounted on the inner surface of the TF coils, which can make contact with poloidal vessel re—enforcement rings which are part of the vessel structure. The springs are not normally engaged; they leave an expansion gap when the vessel is in rest position. They engage with the vessel rings only during the vessel excursions that occur during disruptions. This is illustrated in figure 29. The springs are commercially available disc springs with 250mm outer diameter. The expansion gap between the springs and the vessel support rings should be about 15mm. This will allow baking of the vessel at 300°C without the vessel touching the springs.

Because the springs are normally not engaged with the vessel, they do not have to be thermally insulated from the TF coils. They thermal insulation between vessel and coils can then consist of an evacuated inter—space. With assumed emissivities of 0.2 for the surfaces, the total heat loss across the inter—space is

55kW. This is a small fraction of the steady state liquid nitrogen production capability.

Because the vessel contains poloidal bellows, and is thus not toroidally stiff, the possibility exists of slight misalignments of in—vessel components as limiters and divertor components with respect to the plasma. These misalignments, which will be of the order 1mm, will lead to an uneven distribution of heat loads on these components. Fine tuning of the vessel position can be achieved by fitting of hydraulic actuators and springs on the vessel ports. However, these can only translate the vessel. A further degree of freedom in the alignment can be gained by adjusting the current in individual TF coils. Parallel resistors, adjustable on a day to day basis, can be fitted to the TF coils. The magnitude of the field corrections will be small; it is known from JET, that even field ripple can lead to observable damage modulation on well—aligned low field side belt limiters [20].

In—vessel components. The basic protection of the vacuum vessel will consist of carbon tiles. These tiles will preferably be cooled through the first wall, ie. with cooling channels that are external to the vacuum chamber. A number of poloidal limiters will provide further protection for the ICRH antennas and other in—vessel components.

ICRH antennas. The ICRH antenna system is a uniform array of 16 structures, located one per vessel sector in the locations between TF coils which are connected by shear panels. The vertical location will be in the machine mid—plane. (An alternative scheme, with 32 antennas, where the antennas are located above the mid—plane, is also considered. A 32 antenna set would optimise capabilities for fast wave current drive). The vertical length of the antennas is 2m. The antennas require a poloidal space of 400mm and a radial depth of 30mm. A modular housing for the antennas should be integrated with the vacuum vessel, such that the antenna front surface does not protrude more than a few cm in front of the first wall. Disruption forces on the antenna should be directly transferred to the vessel, and the vessel and antenna cooling should be integrated. The design for the antennas in HLT is a $\lambda/2$ antenna, supported mechanically and terminated electrically at either end by reactive terminations (coils) that are connected to the vacuum vessel. This antenna design does not require electrical insulation material in places exposed to the full.

8. CONCLUSIONS

In this paper, a preliminary design proposal for a tokamak of medium size (R = 3.4m) has been described. The machine, HLT, offers a high performance; a plasma current of 20MA, at a toroidal field of 8T, can be sustained for 40s by inductive current drive. This performance will allow the main physics issues, relevant to a thermonuclear reactor, to be addressed. HLT has a geometry similar to that of JET, and has a similar auxiliary heating power of about 40MW ICRH and NBI. Predictions for the performance of HLT can therefore be made more credibly on the basis of JET results. Important elements of the research programme will therefore be the achievement of ignition, the sustainment of the burn through the removal of ashes and the control of impurities, and the stabilisation of the burn both in the ignited regime and in sub–ignited regimes at reduced plasma current. In the sub–ignited regime, the plasma current can be inductively sustained for 90s, at 15MA, and with a toroidal field of 7T.

A second major research topic, for which HLT is well suited, is the development and optimisation of non–inductive current drive, both in an experimental D–D research phase, and in a D–T phase under realistic thermonuclear conditions. The reference condition for current drive development work is a toroidal field pulse length limit of 500s at 3.5T. This limit is not fundamental, but is determined by the size of the reservoir of cooling energy. The limit can be increased at low investment cost. At the 3.5T toroidal field, current drive can be demonstrated with plasma currents up to 7 or 8MA.

In parallel, a technological research programme can be carried out. Elements of this programme should be the development and optimisation of divertor components capable of accepting high heat loads, development and testing of experimental blanket modules that can be fitted in the ports of the machine, and material tests.

As regards the programme in a deuterium–tritium fuel mixture, it should be noted the first phase of the experimental program will be carried out in deuterium or hydrogen plasmas. The aim is the full commissioning of the device, at maximum toroidal field and plasma current, with about 50% of the powerload that will exist in ignited conditions. This phase will also be used to produce the plasma condition that will produce ignition when reproduced with a deuterium–tritium fuel mixture.

It is expected that HLT will achieve and will be operated in the H mode confinement. At a toroidal field

of 8T, an H mode threshold of about 30MW was predicted on the basis of extrapolation from JET data. This is within the capability of the additional power on the machine. Simple extrapolation from JET H mode data shows that a considerable ignition margin exists in H mode operation.

Preliminary transport calculations show that extrapolating the L mode confinement, using the Rebut—Lallia and Lackner—Gottardi scalings respectively, there also is a margin for ignition. It was shown that ignition is still marginally possible in L mode with Kaye—Big confinement scaling, if plasma purity can be maintained.

HLT uses relatively conservative engineering. The toroidal field coils are liquid—nitrogen cooled, and have a pure copper conductor in a stainless steel casing. The axial stress in the TF coil set does not exceed 180MPa. Crucial to the high current, long pulse capability of the machine is the high power active pressurised liquid nitrogen cooling system. The TF coils are maintained at a temperature below 105K, up to the highest coil currents. This allows one to make full use of the increase of strength of copper at cryogenic temperatures. With this system, the pulse length restriction of the toroidal field coil set depends only on the size of the cooling energy reservoir, which can be increased at low cost.

The total neutron production during a six years D—T research program in HLT was estimated at $2\ 10^{25}$ The neutron fluence implies that a neutron shield is required between the first wall and the toroidal field coils, in order to prevent damage to the coil interturn insulation, and in order to prevent an increase in resistivity of the coil under the accumulation of neutron—induced crystal lattice defects. The shield in HLT consist of between 100 and 150mm of tungsten or lead, in the form of pellets. The shield, and the vacuum vessel, are water—cooled.

ACKNOWLEDGEMENTS

Inspiration for the design of HLT has been obtained from the design of, and the experience gained on, the JET tokamak and the high field tokamaks FT and FTU. Many of the extrapolations made in this paper are made on the basis of data obtained on and published by JET. We are therefore grateful to JET's designer and director, Dr. P.H. Rebut. We are especially grateful for the help and encouragement received from Ing. R. Andreani. We are also grateful for discussions with Dr. L. Pieroni, Dr. A. Sestero, Dr. F. Orsitto, Dr. E. Barbato, Dr. G.B. Righetti, Dr. R. Bartiromo, Ing. S. Ciattaglia and Dr. A. Taroni. We further acknowledge discussions with, and help received from, colleagues at the JET and ENEA—Frascati laboratories. The comments from engineers of Ansaldo Ricerche on some aspects of the engineering of HLT were greatly appreciated.

REFERENCES

[1] Coppi, B., Migliuolo, S., Pegoraro, F., Porcelli, F., Phys. of Fluids B 2 (1990) 927.

[2] Schissel, D.P., DeBoo, J.C. et al., Tubbing, B.J.D. et al., 'H Mode Energy Confinement Scaling from the DIII—D and JET Tokamaks', accepted for publication in Nuclear Fusion.

[3] Cordey, J.G. et al., 13th Int. Conf. on Plasma Phys. and Contr. Nucl. Fus. Res., paper IAEA—CN—53/F/3—19.

[4] Tanga, A., Behringer, K.H., Brusati, M., Costley, A.E., Denne, B., Nucl. Fus. 27 (1987) 1877.

[5] Keilhacker, M., and JET team, Proc. 12th Int. Conf. on Plasma Phys. and Contr. Nucl. Fus. Res., 1 (1988) 159.

[6] Tanga, A., and JET team, 13th Int. Conf. on Plasma Phys. and Contr. Nucl. Fus. Res., paper IAEA—CN—53/A—4—1.

[7] Thomas, P.R. and JET team, ibidem, paper IAEA—CN—53/A—5—3.

[8] Giannella , R., Roccella, M., 'Tokamak approaching Ignition Conditions', to be published in Fusion Technology.

[9] Rebut, P.H., and JET team, Proc. 12th Int. Conf. on Plasma Phys. and Contr. Nucl. Fus. Res., 2 (1988) 191.

[10] Lackner, K., Gottardi, N.A.O., Nucl. Fusion 30 (1990) 767.

[11] Duechs, D.F. et al., II nd Eur. Theory Meeting, Varenna, 7—9 Dec. 1987.

[12] 'The JET project, design proposal for the Joint European Torus', EUR5516e, Office for Official Publications of the European Communities, POB 1003, Luxemburg, 1976.

[13] Rebut, P.H., Keen, B.E., Fusion Technology, 11 1 (1987) 13.

[14] Huguet, M., Dietz, K.J., Hemmerich, J.L., Last, J.R., Fusion Technology, 11 1 (1987) 43.

[15] Moses, R.W., Young, W.C., Proc. 6th Symp. Eng. Probl. Fusion Res., IEEE, New York, (1976) 917.

[16] Bayazitoglu, Y., Ozicik, M.N., 'Elements of Heat Transfer', McGraw—Hill, New York, 1988.

[17] Thompson, M.W.,'Defects and Radiation Damage in Metals', Cambridge University Press, Cambridge, 1969.

[18] Conn, R., in 'Fusion' (Teller, E., et al.), Academic Press, New York, 1981.

[19] Gibson, A., private communication.

[20] Dietz, K.J., and JET team, in Plasma Physics and Controlled Fusion (Proc. 17th Eur. Conf., Amsterdam), to be published.

TABLE 1

MAIN MACHINE PARAMETERS

Major radius	3.405	[m]
Minor radius	1.2	[m]
Elongation	2.0	
Configuration	— low field side discrete limiters	
	— single null divertor	
	— double null divertor	
Auxiliary heating power	ICRH, 20MW, 60 to 95MHz	
	NBI 20MW, ion energy 140keV to 160keV	
	LH 35MW	

OPERATIONAL SCENARIOS

	high performance	long pulse	
Research issues	— ignition	— steady—state current drive	
	— burn—control	— long—pulse divertor operation	
	— ash—removal	— impurity control	
Toroidal field	8.0	3.5	[T]
Plasma current	20	7	[MA]
Fuel	D—T	D—D, D—He—3	
Heating	NBI, ICRH	NBI, ICRH, LH	
Flat top duration	40	500	[s]
Safety factor $q_{\psi,95}$	3.8	3.8	
Divertor connection length	25	26—60	[m]
Nuclear power	$\leq$ 500		[MW]

TABLE 2

MAIN ENGINEERING PARAMETERS

TF COILS	
Maximum toroidal field	8.3 [T] at 3.405m radius
Number of TF coils	32
Shape of TF coils	bending free, with stress transition
Cross–section of TF coils	copper conductor, with stainless steel casing
Conductor material	high–purity oxygen–free copper
Max. current density	55 [MA/m^2]
Operating temperature	70 to 105 [K]
Cooling system TF coils	closed–loop 20 bar pressurised liquid nitrogen
Maximum stress on copper	180 [MPa]
CENTRAL SOLENOID	
Outer radius of central solenoid	1.4 [m]
Conductor material	high–purity oxygen free copper
Max. current density	45 [MA/m^2]
Operating temperature	70 to 110 [K]
Cooling system	closed–loop 20 bar pressurised liquid nitrogen
Max. stress on copper	176 [MPa]
VACUUM VESSEL	
Construction	16 sectors, with poloidal bellows
Operating temperature	20 to 80°C
Vessel cooling	water
Thickness of basic vessel	20 [mm]
Re–enforcements	box sections and poloidal rings
Ports	– 16 main horizontal ports
	– 16 smaller horizontal ports at top and 16 at bottom
	– 32 vertical ports at top and 32 at bottom
Suspension	– weight supported via vertical ports
	– disruptions supported against TF coils
NEUTRON SHIELDING	
Material	lead or tungsten, as pellets
Containment	in box sections of vacuum vessel
Cooling	water

TABLE 3

IGNITION MARGIN F IN H MODE, UNDER VARIOUS CONDITIONS AND WITH DIFFERENT CONFINEMENT SCALINGS

Reference	Schissel [2]	Cordey [3]
CONDITION		
Pressure peaking 5, dilution 0.9	3.12	3.6
Pressure peaking 4, dilution 0.8	2.02	2.3

TABLE 4

REFERENCE DISCHARGE SCENARIOS

DISCHARGE TYPE A: High Q sub–ignited or ignited regime

Fuel	D–T	
Toroidal field	8.0	[T]
Plasma current	20	[MA]
Flat top length	40	[s]
Fusion power	500	[MW]
Neutron power	400	[MW]
Neutron production rate	$1.8\ 10^{20}$	$[s^{-1}]$
Average duration	20	[s]
Total neutrons produced	$3.5\ 10^{21}$	
Cooling energy demand (TF)	36	[GJ]
Electrical energy (TF)	41	[GJ]

DISCHARGE TYPE B: Long pulse, sub–ignited regime

Fuel	D–T	
Toroidal field	7.0	[T]
Plasma current	15	[MA]
Flat top length	90	[s]
Fusion quality factor Q	10	
Fusion power	250	[MW]
Neutron power	200	[MW]
Neutron production rate	$0.9\ 10^{20}$	$[s^{-1}]$
Average duration	50	[s]
Total neutrons produced	$4.5\ 10^{21}$	
Cooling energy demand (TF)	35	[GJ]
Electrical energy (TF)	42	[GJ]

DISCHARGE TYPE C: Long pulse, current drive

Fuel	D–D	
Toroidal field	3.5	[T]
Plasma current (non–induct.)	7	[MA]
Flat top length	500	[s]
Cooling energy demand (TF)	35	[GJ]
Electrical energy (TF)	35	[GJ]

TABLE 5

TOTAL NEUTRON PRODUCTION AND WALL LOADING

Total D—T pulses	10000	
Total neutron production	$2\ 10^{25}$	
Total neutron energy	$4.5\ 10^{13}$	[J]
First wall area	350	[m^2]
First wall neutron fluence	$6.0\ 10^{22}$	[neutrons / m^2]
First wall energy fluence	130	[GJ/m^2]
equals	$4.0\ 10^{-3}$	[MW year/m^2]

TABLE 6

SUMMARY OF TF COIL PARAMETERS

Data are specified for the TF coil set unless indicated as per coil.

Data are specified at the maximum toroidal field unless otherwise indicated.

The TF flat top has, in the maximum performance discharge of type A (see table 4), to exceed the plasma current flat top because the TF centering pressure is required during the pre—magnetisation stage.

Max. toroidal field	8.3T at 3.405m	
Flat top duration max. field	60	[s]
Total current, all coils	141	[MA]
Number of coils	32	
Conductor current density	55	[MA/m^2]
Shape of coil	pure bending, with stress transition at top and bottom.	
Outer radius centre of coil	5.05	[m]
Inner radius centre of coil	1.71	[m]
Inner radius of coil	1.45	[m]
Horizontal internal radius	1.41	[m]
Vertical internal radius	2.88	[m]
Cross—section	tape—wound copper, with steel casing.	
Material for conductor	oxygen free, high purity copper	
Material for casing	stainless steel	
Cooling system	20bar pressurised LN_2, active cooling.	
Normal operating temp.	80 to 105	[K]
Cooling hole area of section	0.04	[m^2]
Fluid speed	5.0	[m/s]
Fluid entry temperature	80	[K]
Coolant flow	10000	[kg/s]
Coeff. of heat transfer	8700	[$W/(m^2K)$]
Cooling power	400	[MW] (at 105K copper temperature)
Pressure drop	0.8	[bar]
Pumping power	1.0	[MW]

Continued TABLE 6

Number of turns	22		
Coil inductance	600	[mH]	
Coil resistance (at 100K)	10	[mΩ]	
Coil current	200	[kA]	
Inductive energy	12	[GJ]	
Resistive dissipation	400	[MW]	
Tensile stress in copper	160	[MPa]	(inner leg)
Tensile stress in steel	290	[Mpa]	(inner leg)
Tensile stress in copper	180	[MPa]	(outer leg)
Tensile stress in steel	325	[MPa]	(outer leg)
Max. voltage power supply	6	[kV]	
Max. current	200	[kA]	
Max. power	600	[MW]	
Max. energy from power sup.	41	[GJ]	
Rise time to full field	40	[s]	
Max. cooling energy	36	[GJ]	

TABLE 7

STRESS CALCULATION FOR CENTRAL SOLENOID, IN COMPRESSION

This is the case with toroidal field on, and no current in the solenoid.

The stresses in the copper are corrected for the presence of cooling holes.

Composite stress is according to maximum shear strain energy.

Vertical stresses are neglected.

—ve stress is compressive, +ve stress is expansive.

Build up of model	see figure 27	
Externally applied pressure	125	[MPa] (TF centering pressure)
Young modulus of copper	120	[GPa]
Weakening of copper by cooling	0.85	
Young modulus of steel	200	[GPa]
Current density in copper	0	[MA/m^2]
Max. radial stress in copper	—144	[MPa] (in all layers)
Max. hoop stress in copper	—152	[MPa] (layer 2)
Max. composite stress in layer 1	146	[MPa]
Max. composite stress in layer 2	148	[MPa]
Max. composite stress in layer 3	146	[MPa]
Max. composite stress inner cyl.	325	[MPa] (at inner radius)
Max. composite stress in shell	191	[MPa]

TABLE 8

STRESS CALCULATION FOR CENTRAL SOLENOID, IN EXPANSION

This is the case with the toroidal field on at maximum value, and the maximum current density in the central solenoid. In the expansion case, the solenoid is allowed to detach from the inner cylinder.

Build up of model	see figure 27	
Conditions	see table 7	
Externally applied pressure	125	[MPa] (TF centering pressure)
Weakening of copper by cooling	0.85	
Current density in copper	45	[MA/m^2]
Max. radial stress in copper	−155	[MPa] (layer 3 at outer radius)
Max. hoop stress in copper	157	[MPa] (layer 1, at inner radius)
Max. composite stress in layer 1	172	[MPa]
Max. composite stress in layer 2	176	[MPa]
Max. composite stress in layer 3	174	[MPa]
Max. composite stress inner cyl.	0	[MPa]
Max. composite stress in c. shell	174	[MPa]

TABLE 9

COOLING CALCULATION FOR THE CENTRAL SOLENOID

The case presented here is for a length of the central solenoid of 5.2m. This is not the full length of the solenoid, but corresponds to the part of the central solenoid that is contained within the straight inner parts of the TF coils. In the outer parts of the coil, the maximum current density is lower. Although these parts will contribute to the flux, and should be included in a full flux calculation, they are not regarded here.

Plasma current	20	[MA]
Current rise time	20	[s]
Flat top time	40	[s]
Average loop voltage	0.2	[V]
Premag. current density	43	[MA/m^2]
Premag rise time	20	[s]
Plasma inductance	7.8	[μH]
Mutual inductance coil to plasma	0.68	[μH] per turn
Coil self inductance	0.76	[μH] per $turn^2$
Mutual inductance vertical field	7.0	[μH] per turn of vertical field coil
Current in vert. field coil	6.5	[MA] at plasma current 20MA
Flux from vertical field	45.5	[Wb]
Solenoid inner radius	1.0	[m]
Solenoid outer radius	1.4	[m]
Length of solenoid	5.2	[m]
Fraction of copper in solenoid	0.8	
Stress limit to solenoid current	45	[MA/m^2]
Diameter of cooling ducts	11.0	[mm]
Total length of ducts	17000	[m]
Fluid speed	8.0	[m/s]
Coolant entry temp.	77	[K]
Pressure drop across coil	1.6	[bar]
Pumping power	400	[kW]
Heat transfer coefficient	13000	[$W/(m^2\ K)$]

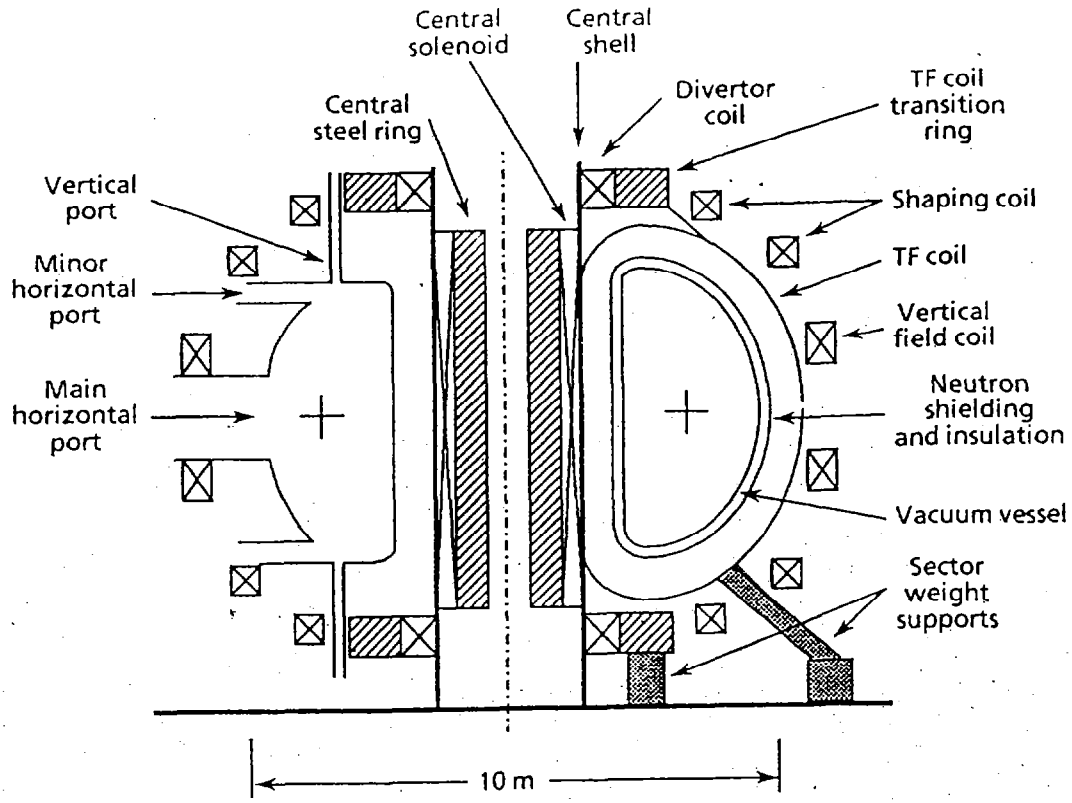

Fig. 1 – Vertical cross-section through the HLT device. The main components are indicated

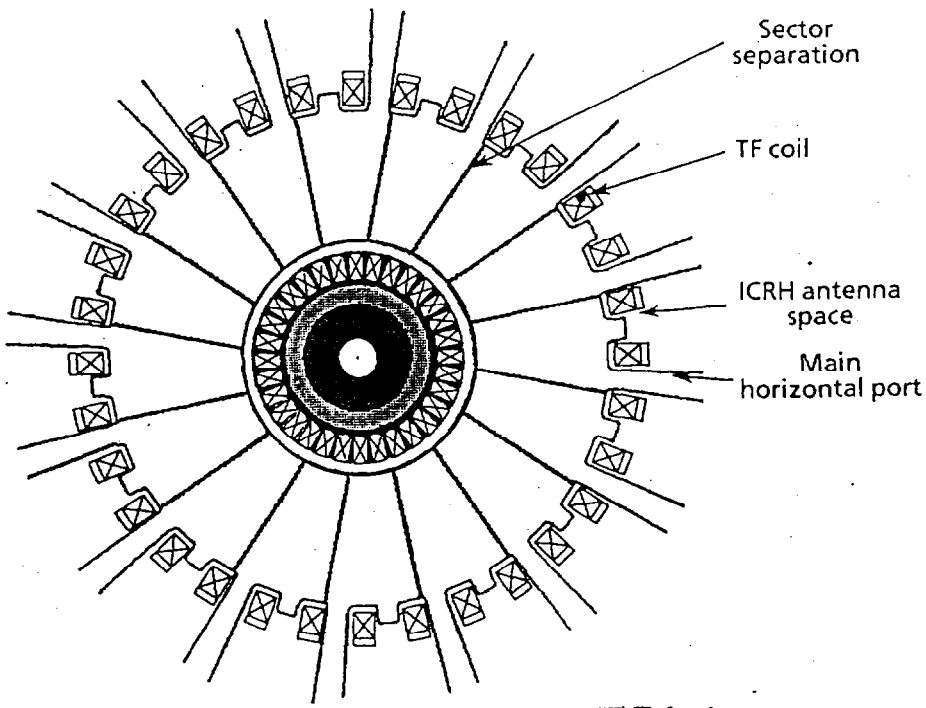

Fig. 2 – Horizontal mid-plane cross section through the HLT device

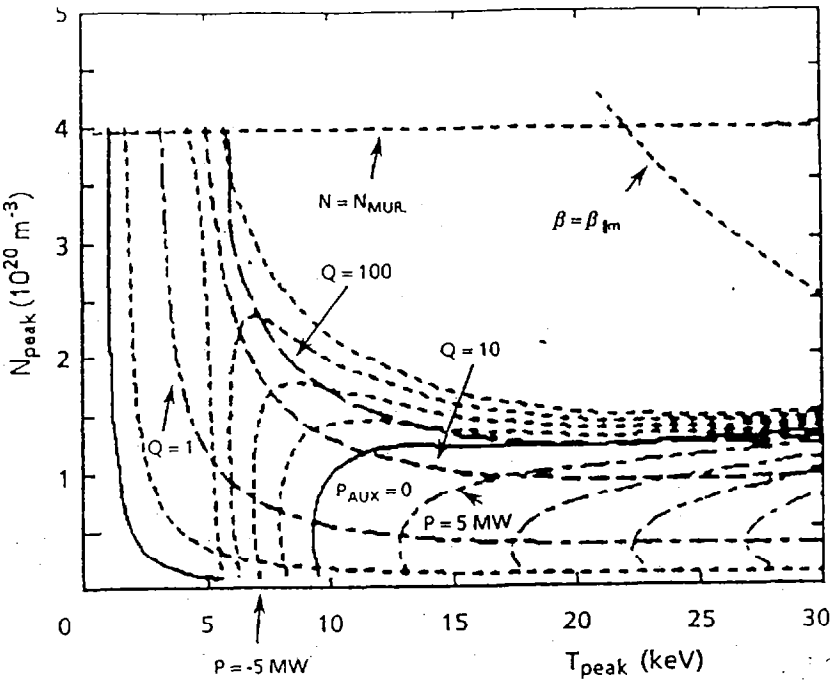

Fig. 3 – POPCON plot for HLT, using Rebut-Lallia global scaling. The vertical axis shows the peak value of the plasma electron density, the horizontal axis shows the peak value of the plasma temperature. The value of the effective ion charge Z_{eff} is 1.0

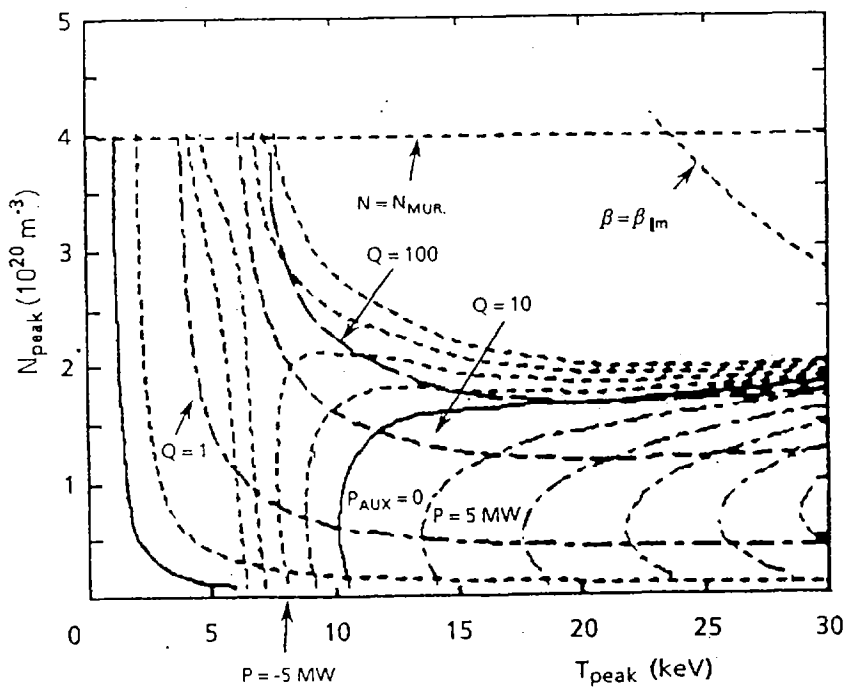

Fig. 4 – As Fig. 3, but for $Z_{eff} = 1.5$

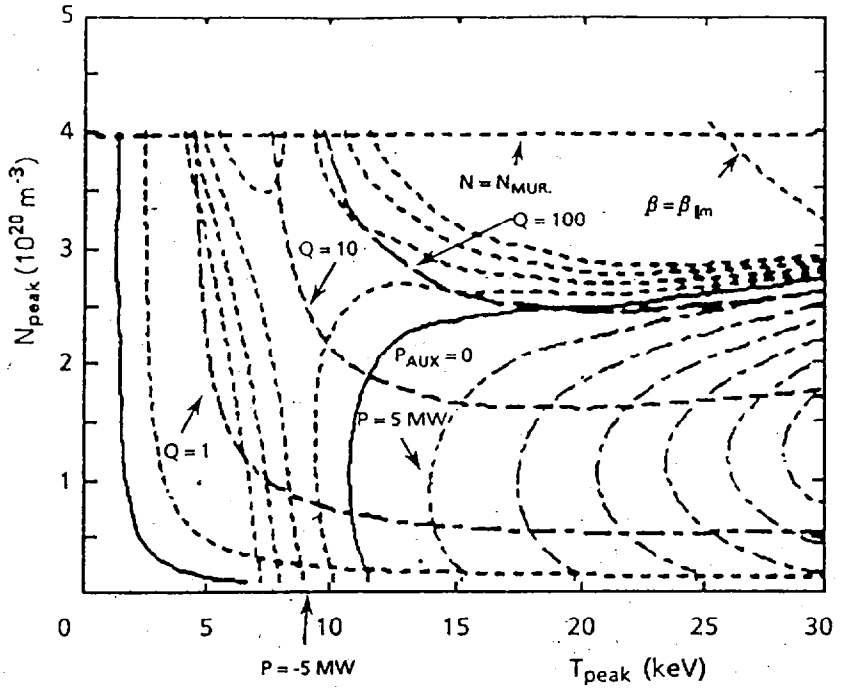

Fig. 5 – As Fig. 3 and 4, but for $Z_{eff} = 2.0$

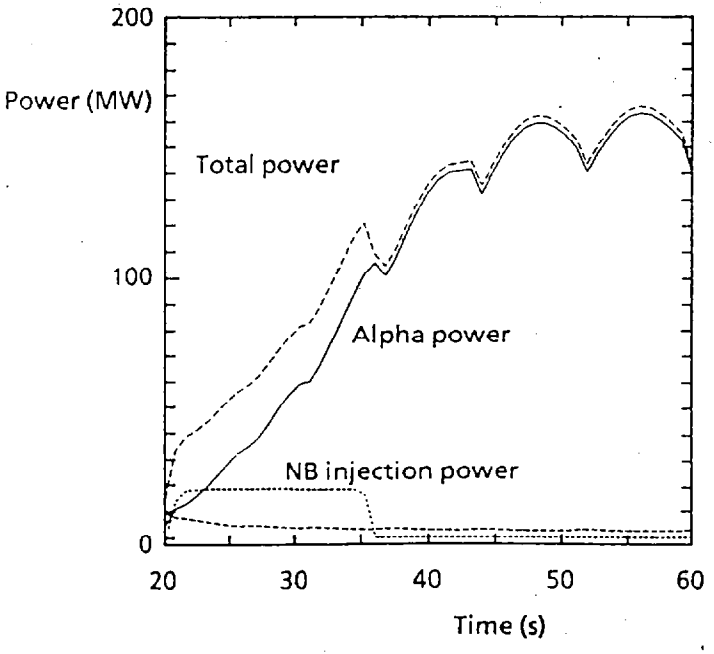

Fig. 6 – Time evolution of the ohmic power, NBI injected power, α particle power, and total input power (NBI plus ohmic plus α power

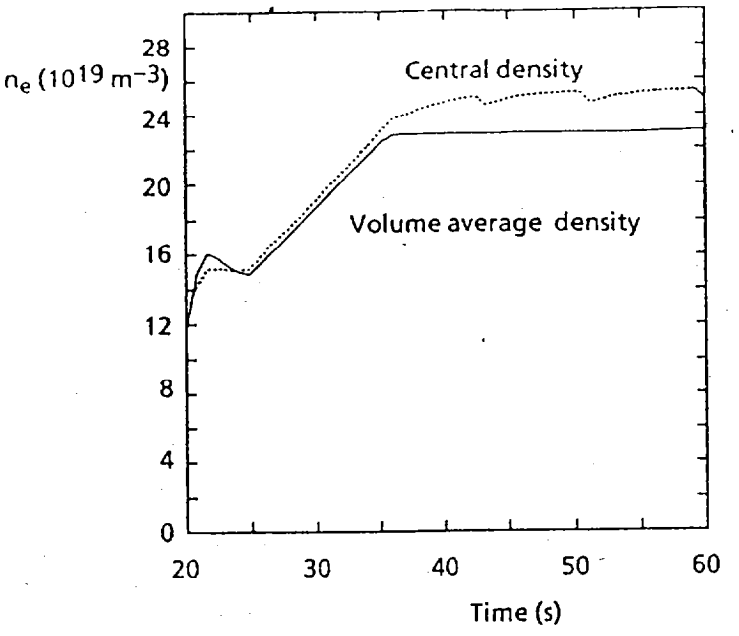

Fig.7 – Time evolution of the volume-averaged density and of the central plasma density

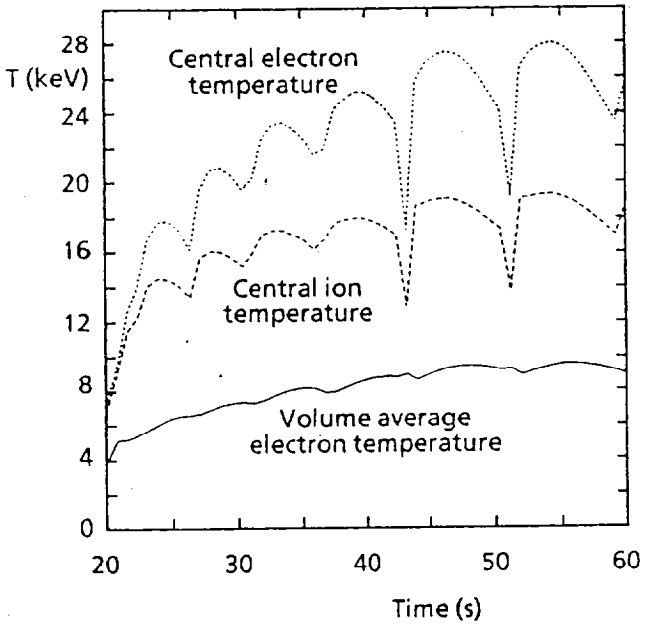

Fig. 8 – Time evolution of the central electron temperature and central ion temperature

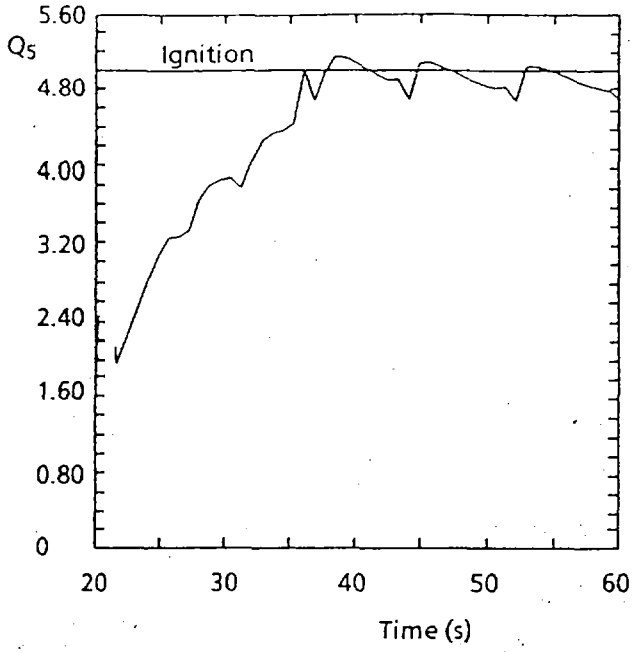

Fig. 9 – Time evolution Q_5 (equals the ratio of total fusion power to total input power (ohmic plus NBI)). Ignition occurs when Q_5 reaches a value of 5

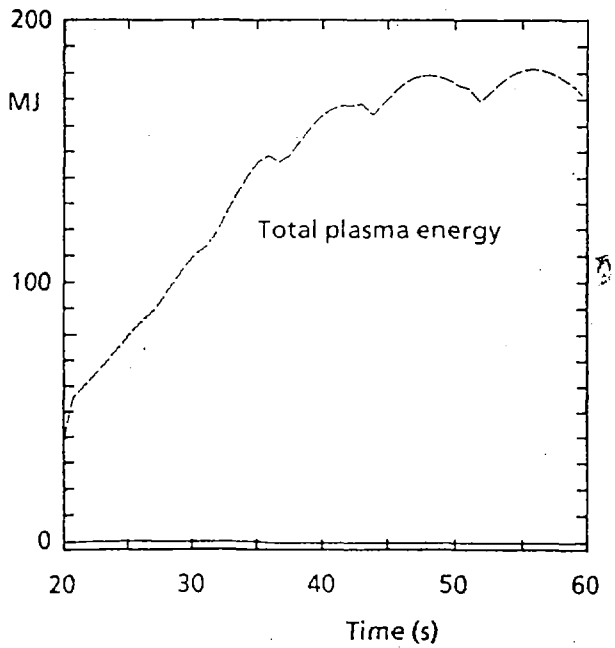

Fig. 10 – Time evolution of the total plasma thermal stored energy. Fast particles are not included

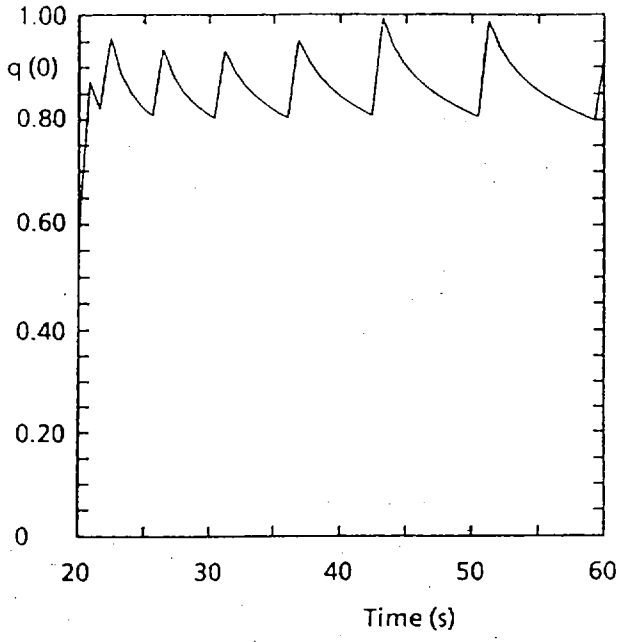

Fig. 11 – Time evolution of the central value of the safety factor q

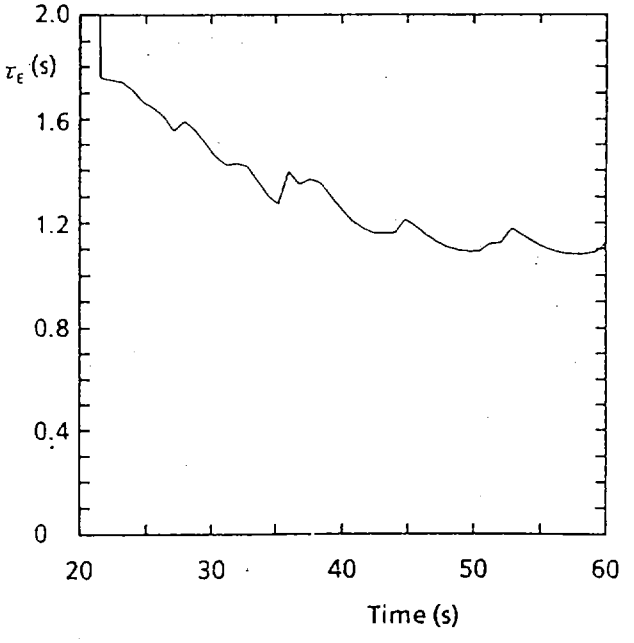

Fig. 12 – Time evolution of the global energy confinement time

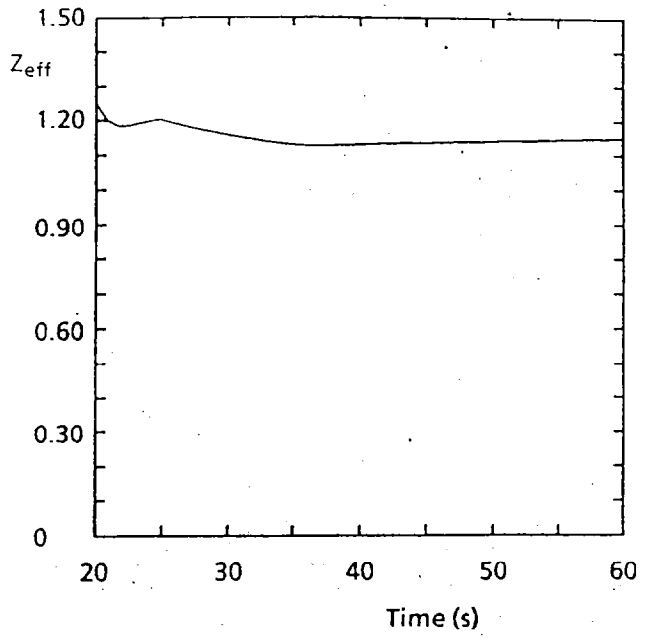

Fig. 13 – Time evolution of the effective ion charge Z_{eff}

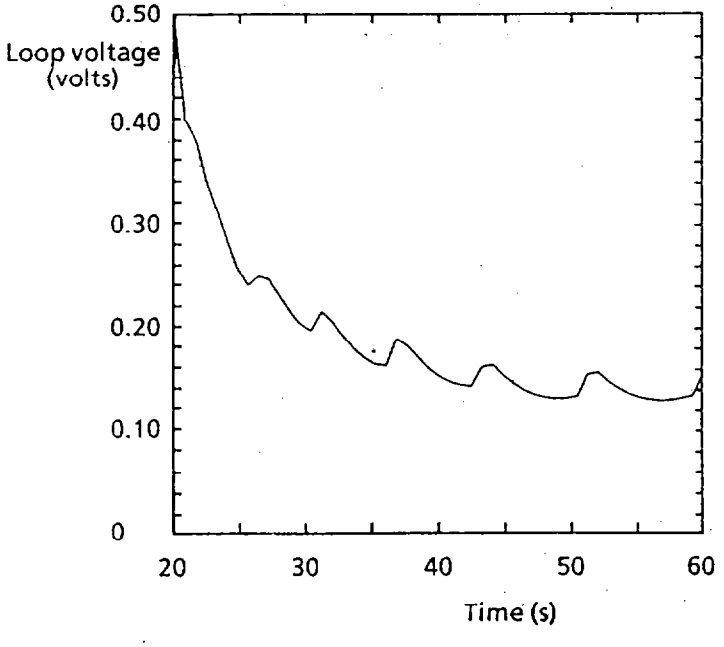

Fig. 14 – Time evolution of the resistive loop voltage

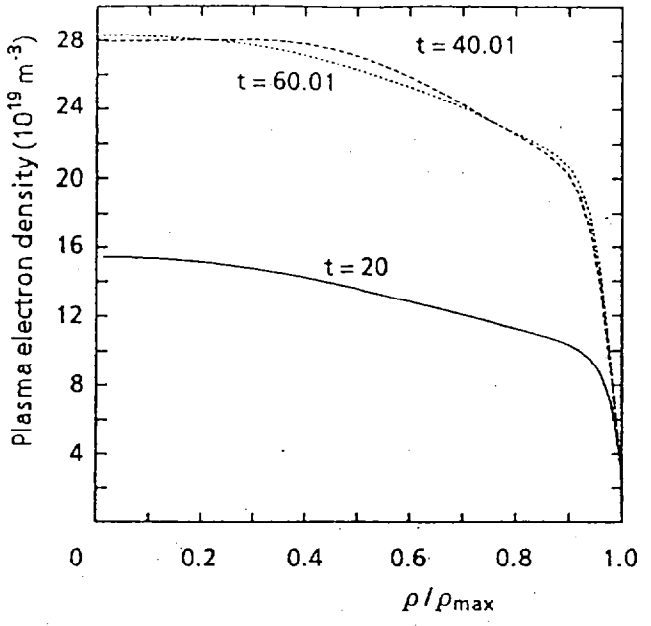

Fig. 15 – Plasma electron density profiles vs the flux normalised radius at times 20 s, 40 s and 60 s

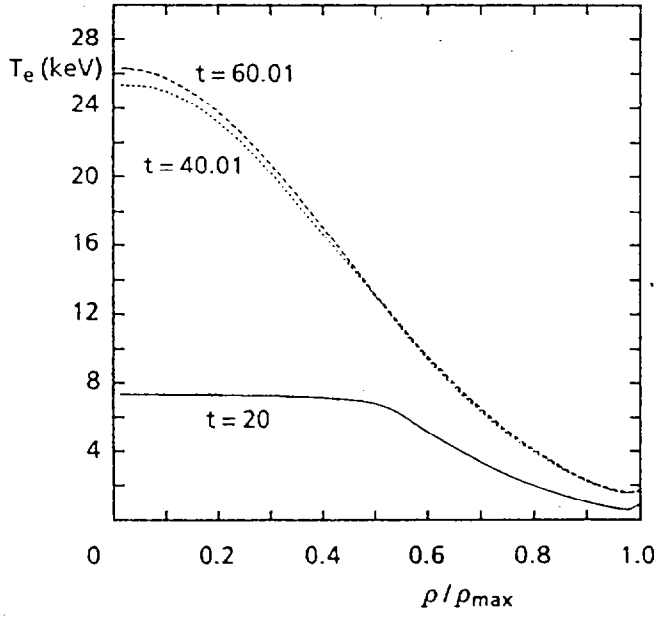

Fig. 16 – Electron temperature profiles vs flux normalised radius, approximately at the peak of the sawtooth, at times near 20 s, 40 s and 60 s

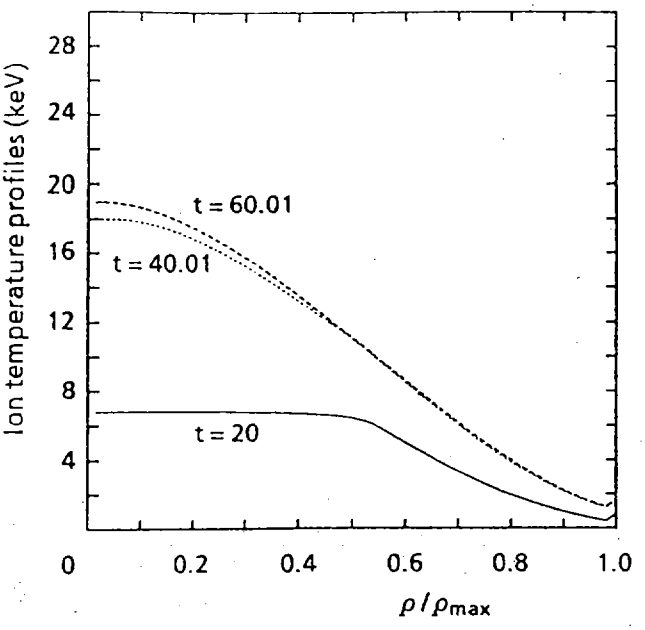

Fig. 17 – Ion temperature profiles, vs flux normalised radius, approximately at the peak of the sawtooth, at times near 20 s, 40 s and 60 s

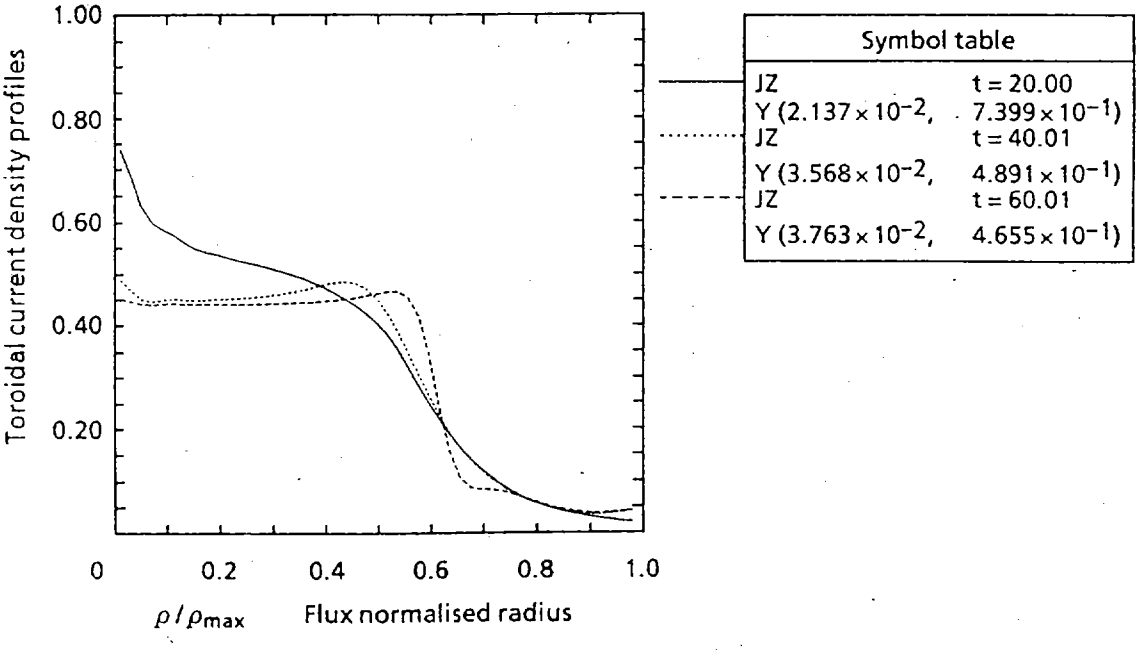

Fig. 18 – Radial profile of the toroidal current density

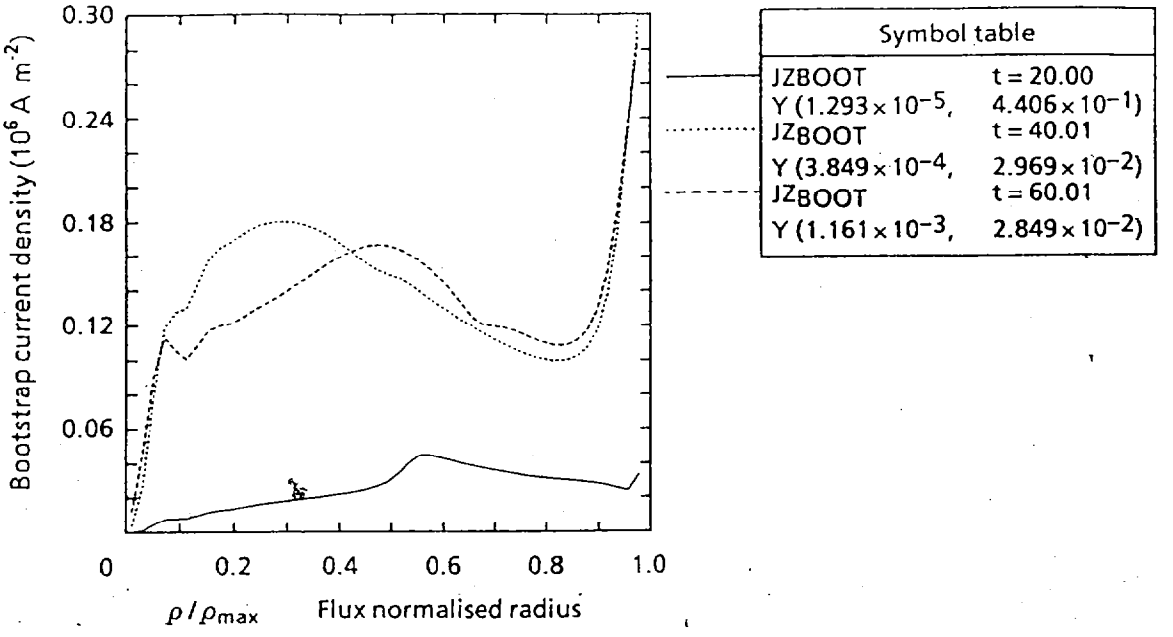

Fig. 19 – Radial profile of the bootstrap current density

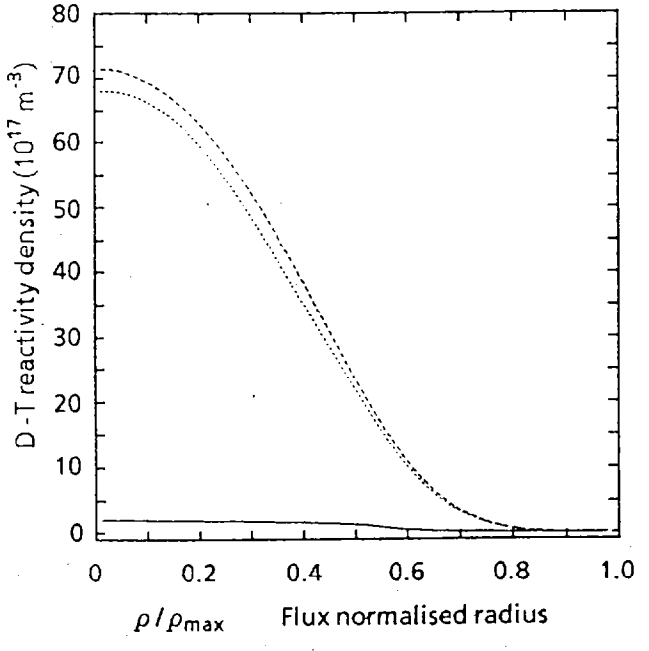

Fig. 20 – Profiles of the D-T reactivity density vs flux normalised radius, at times 20 s, 40 s and 60 s

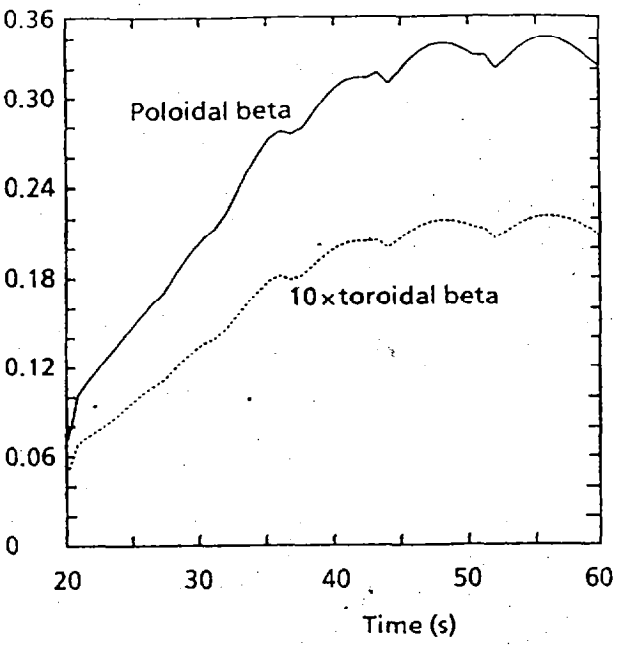

Fig. 21 – Time evolution of the toroidal and poloidal β

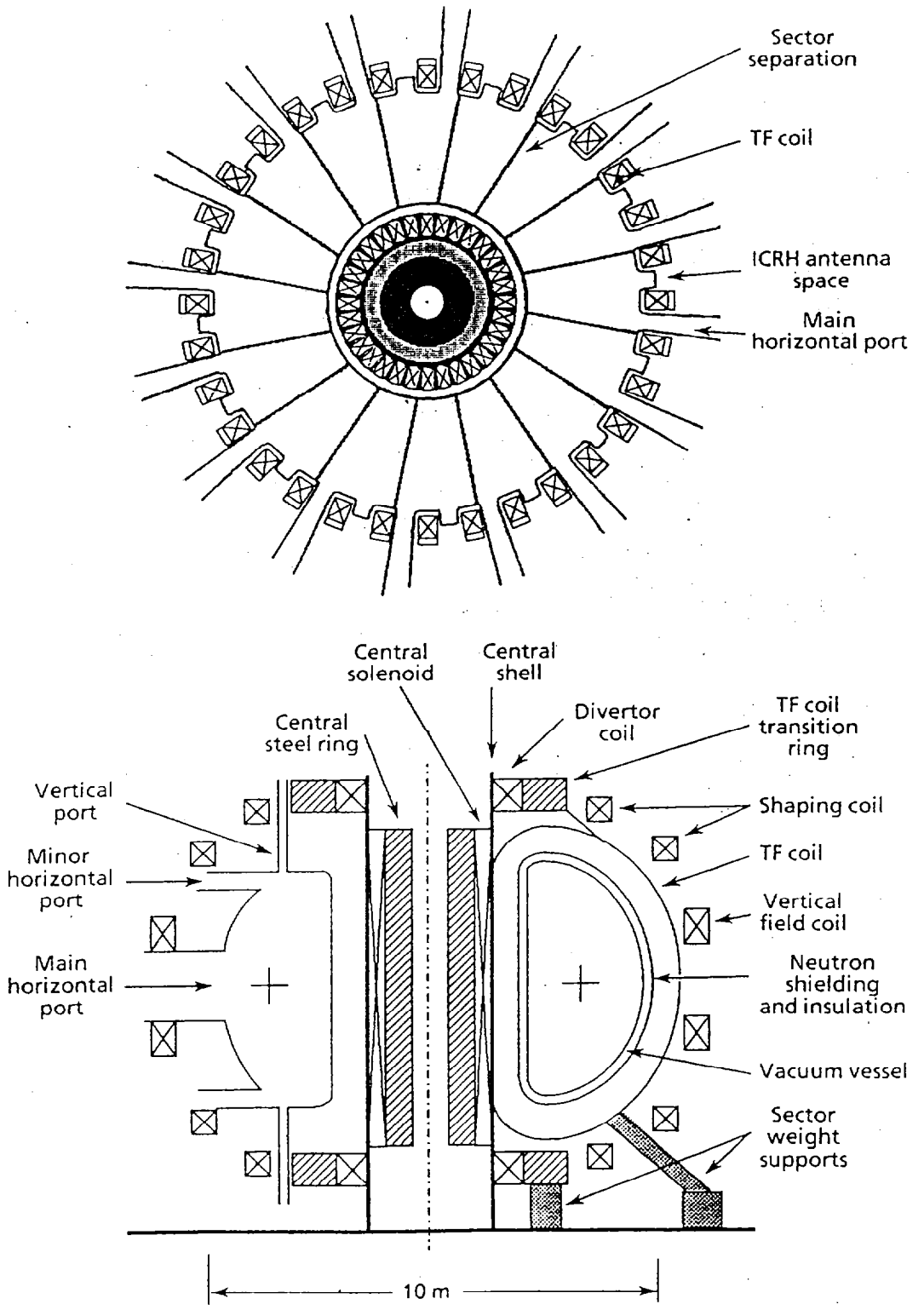

Fig. 22 – Horizontal and vertical cross- sections through HLT the main components of the load assembly are indicated. The lines marked sector separation are the projection in the horizontal mid-plane of the poloidal bellows between sectors of the vacuum vessel. The shear panels and bar connections between the TF loop. The central solenoid loop is similar

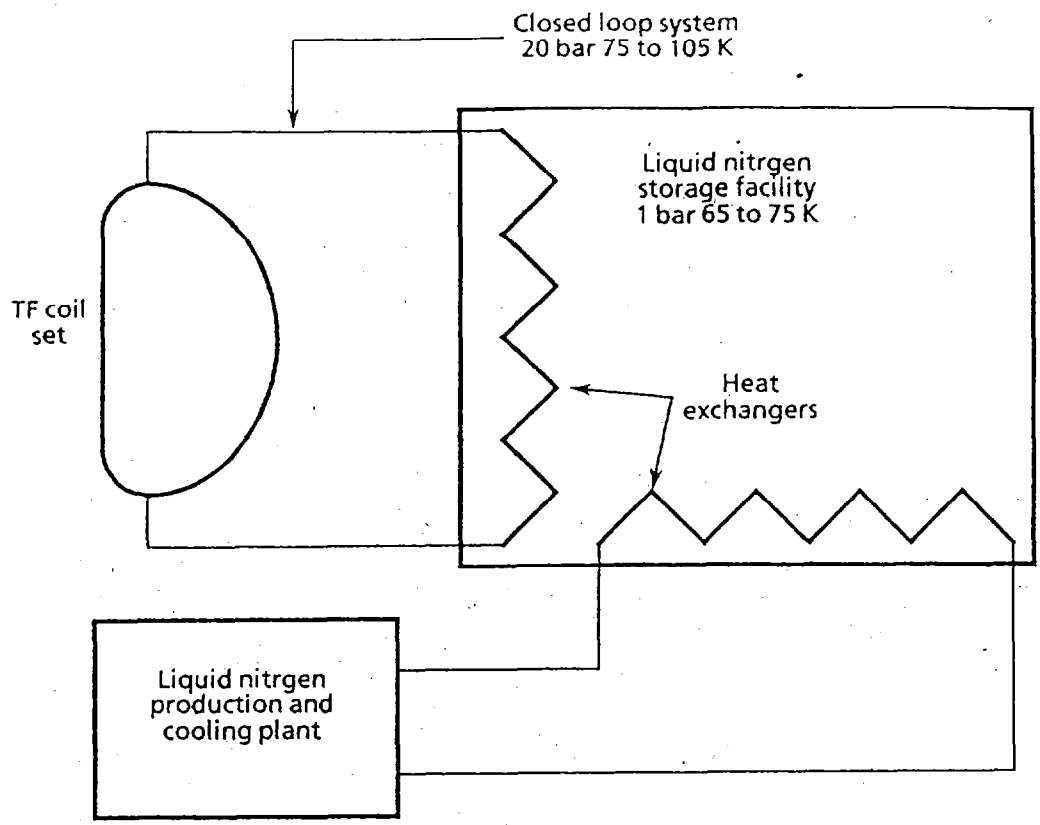

Fig. 23 – Concept of the 20 bar

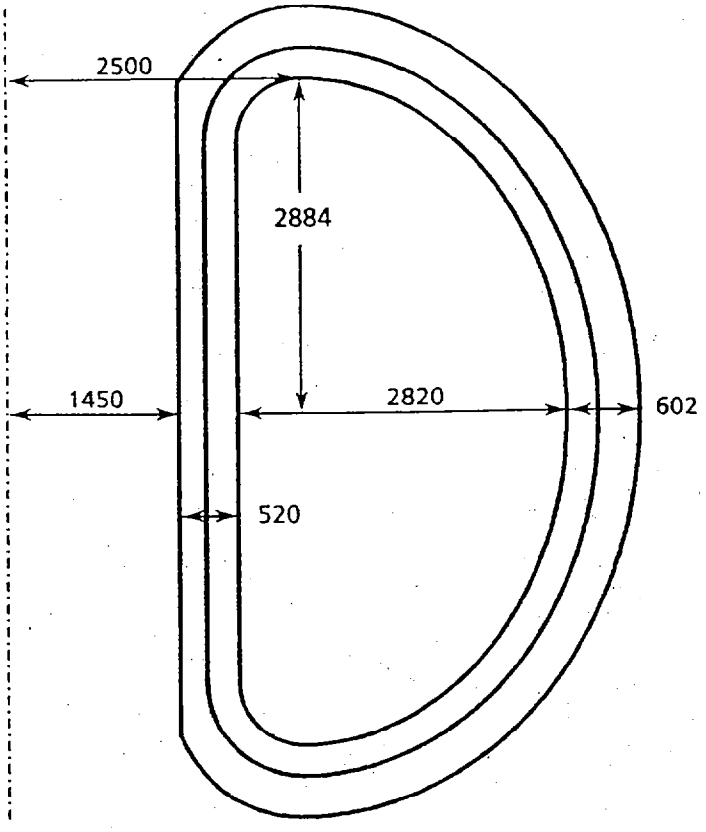

Fig. 24 – Main dimensions of the toroidal field coils

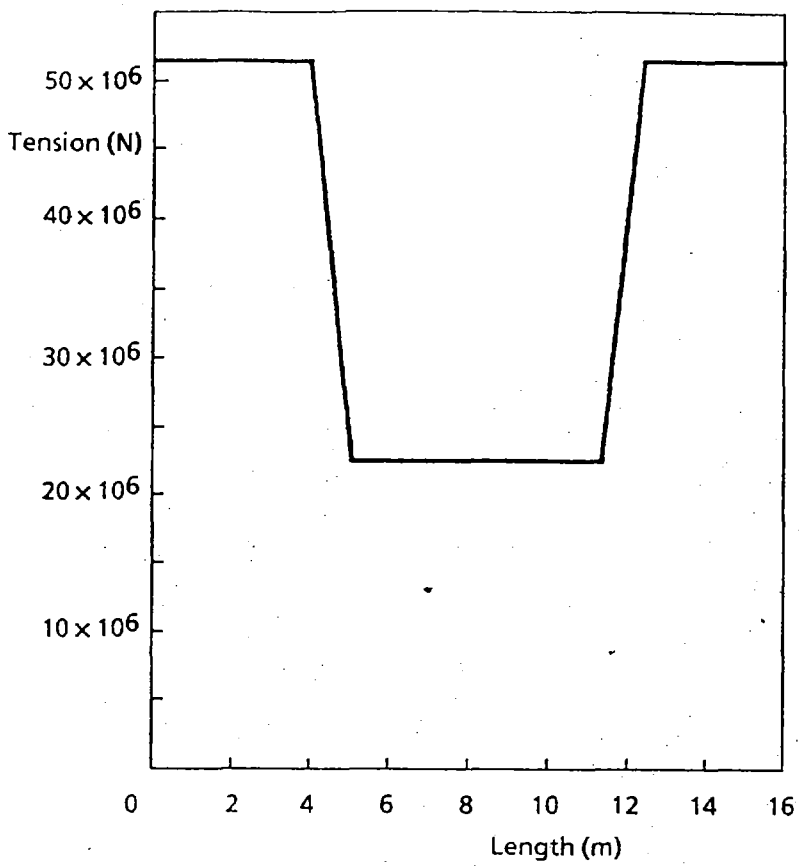

Fig. 25 – The total tensile force in the TF coil as a fucntion of arc length. The origin of the x-rays corresponds to the outer midplane point of the coil

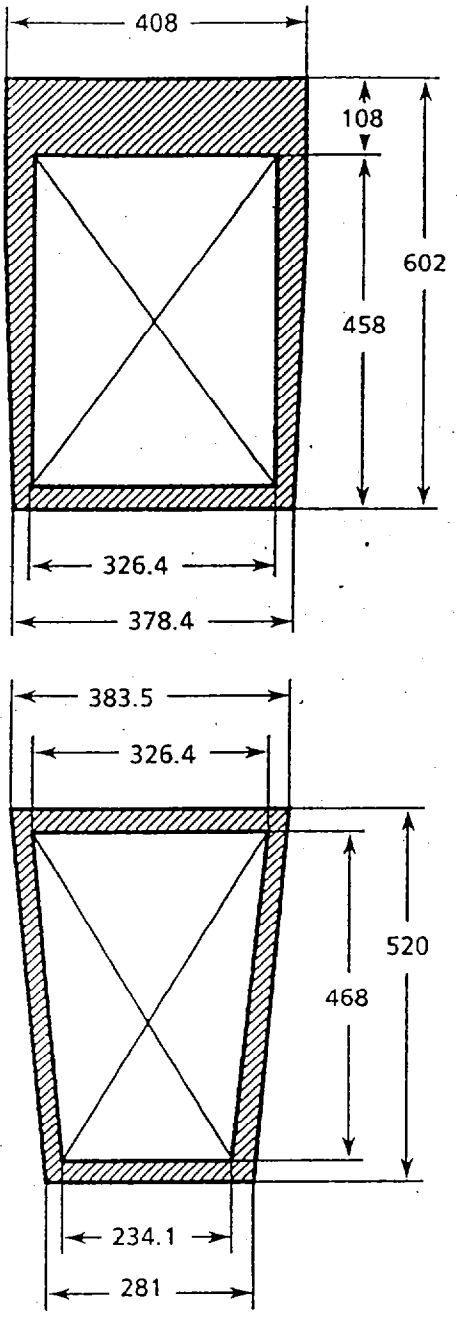

Fig. 26 – Cross-sections of the TF coils. The upper figure shows the low field side cross-section, the lower figure the high field side cross-section. The sides of the low field side cross-section are tapered in order to maximise horizontal port space. The areas of the components are as follows:

high field side: copper 0.08 m^2, steel 0.04 m^2, cooling 0.04 m^2, insulation 0.011 m^2

low filed side: copper 0.10 m^2, stell 0.09 m^2, cooling 0.04 m^2, insulation 0.013 m^2

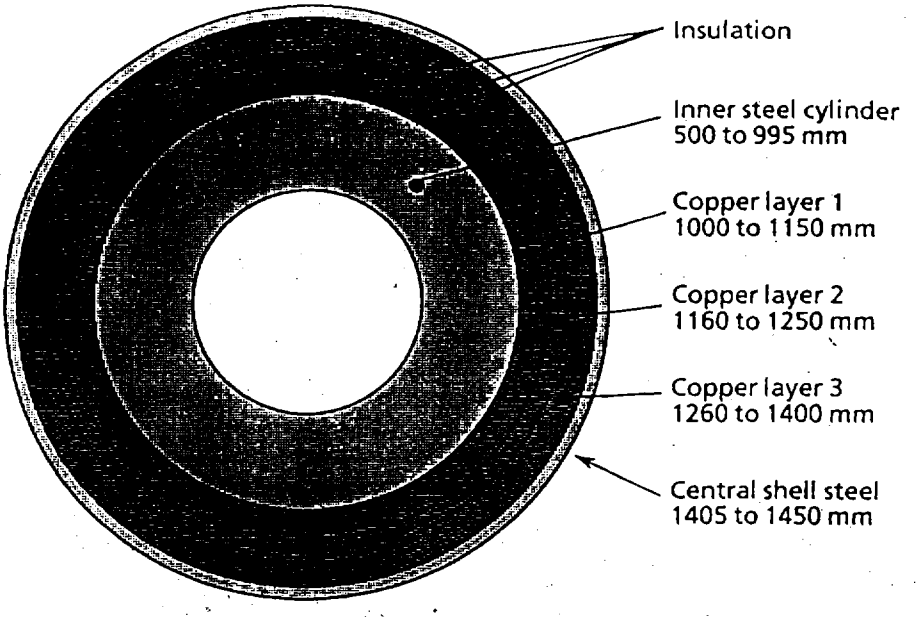

Fig. 27 – Model for the calculation of the stresses in the central solenoid

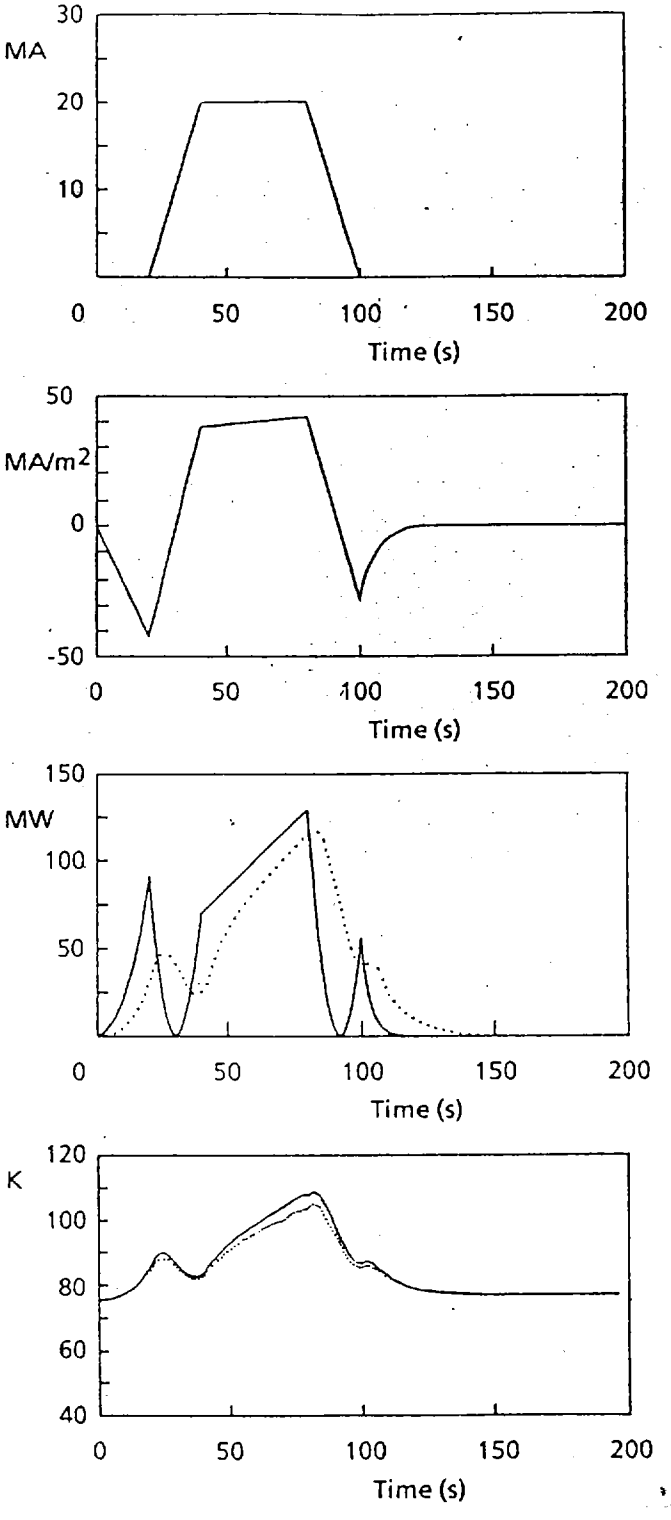

Fig. 28 – Cooling calculation for the central solenoid. Shown are: a) the plasma current for the maximum performance discharge (20 MA with 40 s flat top), b) the current in the central solenoid derived with a simplified flux model, c) the resistive dissipation and the cooling power, d) the temperatures of copper and of exit coolant. For this example, the stress limit on current density (45 MA m2) and the colling limit (110 K), are reached simultaneously at the end of the flat top.

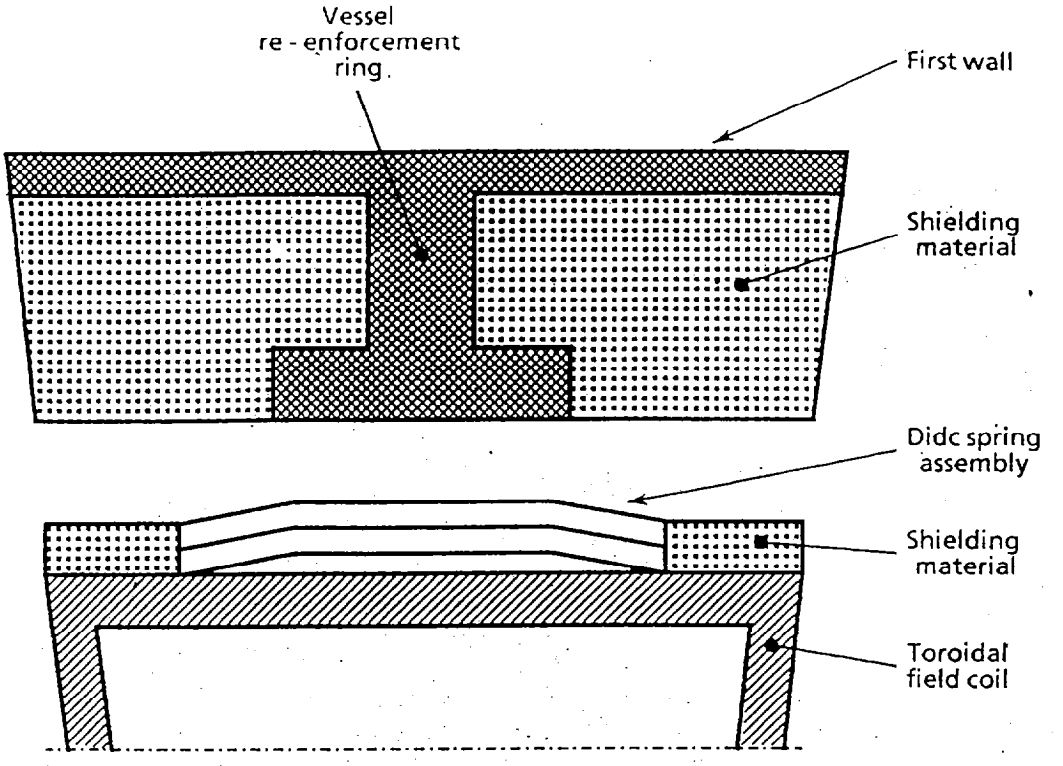

Fig. 29 – Location of the disruption damping springs, poloidal vessel re-enforcement rings and the neutron shielding. Shown is a horizontal cross-section at the high field side of the machine

Edito a cura dall'ENEA, Direzione Centrale Relazioni.
Viale Regina Margherita, 125 - Roma
Finito di stampare nel mese di giugno 1991
Fotoriproduzione e stampa
a cura della «Casa della Stampa»
Via Empolitana 120/C - Tivoli (Roma)